https://doi.org/10.1070/RCR5028

# Effect of pressure on the structure of multispin complexes

**Galina V. Romanenko, Gleb A. Letyagin, Victor I. Ovcharenko**

*The Institute International Tomography Center of the Siberian Branch of the Russian Academy of Sciences,*
*ul. Institutskaya 3a, 630090 Novosibirsk, Russian Federation*

Changes in the hydrostatic pressure may significantly affect the spin dynamics of magnetically active compounds. Hence, objects exhibiting spin transitions have attracted attention of researchers in different fields. Since these transitions are reversible and do not cause the chemical decomposition of the compounds, spin state conversions can be responsible for the functional activity of materials as data storage media, external stimulus sensors or actuators for certain solid-state processes. Moreover, multispin compounds can demonstrate specific structural dynamics that is not inherent in diamagnetic compounds, which is of independent interest. The review presents the analysis of recent data on the effect of hydrostatic pressure on the crystal structure and magnetic properties of metal complexes with organic diamagnetic and paramagnetic ligands, exhibiting spin transitions and valence tautomerism, organic paramagnets and single-molecule magnets.
The bibliography includes 179 references.

## Contents

1. Introduction 1
2. Spin-transition compounds 2
3. Pressure-induced valence tautomerism 5
4. Single-molecule magnets 6
5. Organic paramagnets 6
6. Metal complexes with organic paramagnets. Breathing crystals 8
7. Conclusion 14
8. List of abbreviations and acronyms 14
9. References 14

## 1. Introduction

High-pressure studies of the structures and properties of compounds have attracted increasing attention from researchers in different fields. Previously, this was an area of interest mainly for physicists and geoscientists. These researchers investigated behaviour of materials under shock loading conditions, the properties of compounds and the mineral formation inside the Earth, where the pressure can reach hundreds of gigapascals (140 GPa deep inside the Earth's mantle, 360 GPa in the Earth's inner core; 1 atm $\approx 10^{-4}$ GPa), as well as the electronic structures of highly compressed materials. Currently, various materials are extensively studied at high pressure by chemists [1] and biologists.[2–6] High-pressure studies can reveal unexpected properties of seemingly usual compounds.[1] For example, solid sulfur hydride showed superconductivity (the superconducting critical temperature at 149 GPa is 183 K).[7] An ultrahigh pressure (several hundred gigapascals) allows a significant increase in the critical temperature of transition ($T_c$) to the superconducting state in many compounds. Thus, recently it was found that the C–S–H ternary system became superconducting even at nearly room temperature (287.7 ± 1.2 K) under a pressure of 267 ± 10 GPa.[8] The pressure can cause changes in such properties as luminescence,[9] conductivity and colour (for example, sodium becomes an optically transparent insulator at $P \approx 200$ GPa),[10] and also magnetic properties.[11,12] Application of high-pressure pulses can generate radio-frequency superradiance under the rheological explosion.[13,14] The high-pressure synthesis of novel compounds and the preparation of new polymorphs of known compounds have also attracted the attention of chemists.[15–19]

The field of molecular magnetism and possible applications of single-molecule magnets have been extensively investigated in recent years due to advances in the synthesis of coordination compounds exhibiting magnetic hysteresis at temperatures sufficiently high to make them suitable for technological applications, such as the data storage and the development of devices for spintronics and quantum computing. Meanwhile, the high-confidence prediction of the structures of compounds with specified properties requires comprehensive systematic studies, in which the coordination geometry of the metal ion will be gradually varied through the direct alteration of the structure of ligands or outer-sphere molecules or, alternatively, their crystal pack-

**G.V. Romanenko**. Doctor of Chemical Sciences, Chief Researcher at the Laboratory of Multispin Coordination Compounds, ITC SB RAS.
E-mail: romanenko@tomo.nsc.ru
*Current research interests*: single-molecule magnets, crystal structure, magnetic and structural phase transitions.
**G.A. Letyagin**. Junior Researcher at the same Laboratory.
E-mail: gl@tomo.nsc.ru
*Current research interests*: single-molecule magnets, external stimuli-induced crystal structure transformations.
**V.I. Ovcharenko**. Academician, Professor, Doctor of Chemical Sciences, Head of Scientific Area Molecular Magnets, Head of the same Laboratory.
E-mail: Victor.Ovcharenko@tomo.nsc.ru
*Current research interests*: coordination chemistry, design of single-molecule magnets, organic radicals, spin transitions, magnetochemistry.

Translation: T.N.Safonova

**Received 11 June 2021**

© 2022 Uspekhi Khimii, ZIOC RAS, Russian Academy of Sciences and IOP Publishing Limited

ing. It should be taken into account that the typical change of one $-CH_2-$ unit in a homologous series in organic chemistry (*e.g.*, in changing from the $CH_3$ to $C_2H_5$ group) may be too large and will lead to differences in the packing and the energy of intermolecular interactions, with an unpredictable effect on the magnetic properties.[20, 21] Another approach, which retains the composition of the complex, can be accomplished under the action of external stimuli on the crystal, for example, by varying the temperature, pressure, irradiation, electric field, *etc*. In this case, the experimental conditions can be altered with a small step size, *i.e*., by continuously changing the external stimulus. Crystal structure investigations of compounds by X-ray diffraction (XRD) in a wide temperature range have long been an integral part of studies of magnetically active compounds, because it is often impossible to explain the existence of anomalies in thermomagnetic curves without using X-ray diffraction data.

High-pressure single-crystal structure determination and magnetochemical measurements of magnetically active compounds started three decades ago. These experiments are often performed independently and sometimes at intervals of several years and, besides, magnetic measurements are generally performed using polycrystalline samples.[22, 23] Recent advances in research on high-pressure crystal structures were due to the improvement in the design of diamond anvil cells for experiments using laboratory diffractometers as well as synchrotron and neutron sources.[15, 17, 24–27]

Great attention is currently given to pressure-induced structural transformation of transition metal coordination compounds, exhibiting spin transitions or valence tautomerism, and 3d–4f complexes showing single-molecule magnet behaviour.[11, 18, 28] The external hydrostatic pressure causes changes in the coordination environment of the metal ion. The analysis of these changes allows one to examine in detail the effect of these changes on such properties of compounds as magnetism, electrical conductivity, thermo- and piezochromism. However, this area is still poorly investigated, in particular, for organic paramagnetic materials and respective metal complexes.

The available literature data on these studies are scattered over different sources. This review summarizes the most interesting, in our opinion, recent data on the effect of external hydrostatic pressure on the crystal structures and properties of magnetically active compounds, such as spin-crossover or valence tautomeric metal complexes, organic paramagnetic materials and single-molecule magnets.

The figures presented in the review were prepared by the authors using the data from the publications, identified in the figure legends, and the Cambridge Structural Database (CSD, version 5.42, 2020, update of September 2021).[29]

## 2. Spin-transition compounds

The phenomenon, referred to as spin transition or spin crossover,† is the switching process between the high-spin (HS) and low-spin (LS) states of molecules and is observed for transition metal complexes with the $d^4-d^7$ electronic configuration of the metal ion. More than 90 years have passed since the discovery of the spin-crossover phenomenon by Cambi and Szegö,[30] and hundreds of mono- and polynuclear complexes, exhibiting spin transitions, were synthesized in the solid, liquid or gel state during that time. The properties of these compounds are described on the molecular level in terms of the ligand field theory.[31] The analysis on the macroscopic level is generally performed in terms of the theories of crystal lattice elasticity and electron–phonon interactions.[32] For a great number of compounds of the class under consideration, the effects of temperature, pressure, light and magnetic field on the character of magnetic anomalies were explained and theoretically justified.[33] It is also worth noting that spin transitions can be accompanied, apart from the changes in the magnetic susceptibility and colour, by changes in the dielectric and mechanical properties of the compounds.[34–38]

Materials based on complexes capable of switching between the HS and LS states have useful properties favourable for their potential use. These properties include the following: [11, 12, 39, 40]

— the spin transition can occur even in systems of sizes down to a few nanometers;

— the switching of the spin state can occur at room temperature;

— the switching is accompanied by ultrafast (within hundreds of femtosecond) changes in electronic states;

— compounds exhibiting hysteresis effects are potentially favourable for the design of data storage devices;

— compounds offer wide possibilities for the chemical design of new compounds with desired properties.

Spin transitions are usually detected by magnetochemical measurements or spectroscopic methods, such as optical absorption spectroscopy, Mössbauer spectroscopy and EXAFS (extended X-ray absorption fine structure) spectroscopy; measurements of electrophysical properties are used much more rarely.[36, 41] High-pressure structural studies are even more scarce. For example, the pressure effect on the crystal structure was addressed in a limited number of studies concerning the most well-characterized $Fe^{II}$ compounds, containing the $\{FeN_6\}$ unit and exhibiting spin-crossover behaviour, the data for which are available in the CSD.[29] Most of these studies were devoted to mononuclear $Fe^{II}$ complexes,[42–48] while the pressure effect on the structures of polymeric complexes was evaluated only in two studies.[27, 49]

In the first approximation, the pressure effect on the spin crossover leads only to a change in the temperature of this transition ($T_c$) due to a change in the enthalpy difference between the HS and LS states ($\Delta H_{HL}$) by the amount of work against external pressure forces during the phase transition

$$\Delta H_{HL}(P) = H_{HS}(P) - H_{LS}(P) \approx \Delta H_{HL}(P = 0) + P\Delta V_{HL} \qquad (1)$$

where $\Delta V_{HL} = V_{HS} - V_{LS}$ is the molar volume difference between the high- and low-spin phases near the equilibrium point.

If at atmospheric pressure the HS and LS phases are in equilibrium at $T_c$, the equilibrium shifts towards the denser phase with increasing pressure in accordance with the Le Châtelier–Braun principle. The change in $T_c$ can be more strictly determined using the Clausius–Clapeyron equation [28, 50]

$$\frac{dT_c}{dP} = \frac{\Delta V_{HL}(P)}{\Delta S_{HL}(P)} \qquad (2)$$

† The terms 'spin crossover' and 'spin transition' are synonyms. Both terms are used in English-language literature concerning the spin-crossover phenomenon.

where $\Delta S_{HL} = S_{HS} - S_{LS}$ is the change in the molar entropy upon the phase transition. The volume of the HS isomer is larger compared to the LS isomer because electrons in the high-spin state are redistributed to antibonding orbitals. Consequently, the metal–ligand distances in the coordination polyhedron of the HS isomer are larger (in divalent iron compounds, the Fe–N bonds are ~0.2 Å longer).[51, 52] The $\Delta S_{HL}$ value is positive and is mainly determined by changes in the vibrational entropy and the spin degeneracy multiplicity.[28] Therefore, the ratio $\Delta V_{HL}/\Delta S_{HL}$, like $\Delta V_{HL}$ and $\Delta S_{HL}$, is also positive. From the positive value of $dT_c/dP$, it follows that an increase in the external pressure causes an increase in the phase transition temperature in accordance with the Clausius–Clapeyron equation.

Based on the analysis of the data available up to 2018, Gaspar *et al.*[28] concluded that most compounds exhibiting continuous spin crossover without hysteresis[53–62] behave as predicted by the Clausius–Clapeyron equation. Thus, the transition temperature is gradually shifted upwards with increasing pressure and the derivative $dT_{1/2}/dP$ (where $T_{1/2}$ is the temperature, at which half of the total amount of spin-changing molecules are in the LS state) is 146–220 K GPa$^{-1}$. This pattern was demonstrated for both mononuclear and polymeric $Fe^{II}$ complexes.[61, 62] For example, variable pressure and variable temperature (150–290 K at 0.101–0.181 GPa) structural study of the polymer $\{Fe(pmd)_2[Ag(CN)_2]_2\}_n$ (pmd is pyrimidine) by neutron Laue diffraction demonstrated that $T_c$ is displaced by ~140 K GPa$^{-1}$ with increasing pressure.[27]

The external pressure not only causes the shift of $T_c$ but also may induce structural rearrangements different from those caused by the cooling of the crystals at atmospheric pressure. A nonlinear dependence of $T_c$ on the pressure and changes in the character of the magnetic properties and(or) the transition to a high-pressure phase may be observed under an external stimulus.[48] Besides, such properties of the crystal as the elasticity modulus and the phonon frequency may be significantly changed, which will be reflected in the $\Delta S_{HL}$ and $\Delta V_{HL}$ values. Since the pressure affects intermolecular interactions, it can lead also to a significant change in the cooperative spin-crossover behaviour.[28, 50, 63, 64] One should not forget about the possible difference in the anisotropy of temperature- and pressure-induced changes in the crystal lattice, due to which the spin state of the $Fe^{II}$ ion may remain unchanged with increasing pressure.[42]

Polymorphism makes it difficult to perform comparative studies of the effects of the temperature and pressure on the spin transition. Thus, four polymorphs (A, B, C and D) are known for $[Fe(abpt)_2(NCS)_2]$, where abpt is 4-amino-3,5-bis(pyridin-2-yl)-1,2,4-triazole. For the polymorphs A, C and D, the temperature-induced spin crossover was observed at atmospheric pressure, whereas this effect for the polymorph B was detected only at a pressure of >0.44 GPa. Only for the polymorph A, the HS → LS structural changes under pressure increase are similar to those observed on cooling.[45, 55] Apparently, this is due to the fact that the structures of the polymorphs C and D contain two crystallographically independent $Fe^{II}$ ions, whereas there is one independent $Fe^{II}$ ion in the polymorph A. Upon cooling, only one $Fe^{II}$ ion undergoes a spin transition in the polymorphs C and D, while another $Fe^{II}$ ion remains in the HS state.

The complex $[Fe(phen)_2(NCS)_2]$, where phen is phenanthroline, is one of the most well-characterized spin-crossover compounds.[44, 65–70] This compound can exist in two modifications, which have somewhat different magnetic properties.[66] This is why there are differences in the description of the properties of $[Fe(phen)_2(NCS)_2]$. Thus, different authors evaluated the spin transition pressure ($P_c$) at room temperature in the range from 0.6 to 1.35 GPa.

Magnetochemical measurements demonstrated that the modification $[Fe(phen)_2(NCS)_2]$-II exhibits an abrupt spin transition ($T_c \approx 176$ K) with a hysteresis at atmospheric pressure.[56, 71] At a pressure of 0.17 GPa and above, the hysteresis disappears and the transition becomes continuous. An increase in the pressure leads to a shift of the temperature dependence of the magnetic properties of this complex to higher temperatures with a rate of 220 K GPa$^{-1}$, the plot of $T_{1/2}$ *versus* the pressure being nearly linear. At 0.57 GPa, the sample is almost completely in the LS state.

The complexes $[Fe(phen)_2(NCS)_2]$-II and $[Fe(btz)_2(NCS)_2]$, where btz is 2,2′-bis(4,5-dihydrothiazine), are isostructural. In the crystal structures of these complexes, the molecules are arranged in layers parallel to the (001) plane. The most significant intramolecular changes in both complexes provoked by pressure increase or temperature decrease are similar: the Fe–N bonds in the $FeN_6$ coordination unit become shorter and the coordination polyhedron adopts a nearly ideal octahedral geometry. The main effect is an increase in the number of short (with distances smaller than the sum of the van der Waals radii of the corresponding atoms) intermolecular contacts. Using the correlation between the fraction of the molecules in the HS state and the unit cell volume, Granier *et al.*[44] succeeded in separating the contributions of the spin crossover and the lattice compressibility to the pressure-induced reduction in the unit cell volume.[44]

Four complexes $[FeL_2(NCS)_2]$, where L is 2,2′-bipyridine (bipy), btz, phen or dipyrido[3,2-*a*:2′3′-c]phenazine (dpp), the former three of which are isostructural, were investigated.[72, 73] All complexes exhibit spin crossover when cooled at atmospheric pressure. In the compound $[Fe(btz)_2(NCS)_2]$, the spin transition is continuous and extended by ~50 K. Consequently, this compound shows spin transition with weak cooperativity. An abrupt spin transition was observed for the other three complexes; $[Fe(dpp)_2(NCS)_2]\cdot py$, where py is pyridine, shows a spin transition with a hysteresis loop of ~40 K width. Hence, it was found that the cooperativity of the spin transition increases in the series

$$[Fe(btz)_2(NCS)_2] < [Fe(bipy)_2(NCS)_2],\ [Fe(phen)_2(NCS)_2] < [Fe(dpp)_2(NCS)_2]\cdot py$$

and it was suggested that it correlates with the strength of intermolecular interactions in the crystal. However, only studies of the high-pressure effect on the crystal structure[28, 48] made it possible to reveal the true cause of high cooperativity of the spin transition in $[Fe(dpp)_2(NCS)_2]\cdot py$ and determine the microscopic mechanisms responsible for the cooperativity of the effect. The complex $[Fe(dpp)_2(NCS)_2]\cdot py$ exhibits negative thermal expansion (NTE) and negative linear compressibility (NLC), which is reflected in the negative sign of the following thermodynamical coefficients:

$$\alpha_i = \frac{1}{l}\left(\frac{\partial l}{\partial T}\right)_P \quad (3)$$

the linear compressibility coefficient (LCC)

$$K_i = \frac{1}{l}\left(\frac{\partial l}{\partial P}\right)_T \quad (4)$$

where $l$ is the size of the body in a certain direction (or the unit cell parameter).

Both inorganic [74, 75] and organic [76] compounds exhibit NTE and NLC. Generally, specific structural motifs are required for the occurrence of NLC. These motifs, in turn, can give rise to a NTE. It is worth noting that the laws of thermodynamics do not require that tthe compound with NLC should exhibit NTE; nevertheless, these properties are often manifested together.

On cooling at atmospheric pressure $[Fe(dpp)_2(NCS)_2]\cdot py$ undergoes thermal spin crossover with a hysteresis loop of 40 K width ($T_c\downarrow$123 K, $T_c\uparrow$163 K).[77] A very abrupt spin transition is accompanied by an isostructural crystallographic phase transition. The HS → LS spin crossover leads to a very small decrease (by 0.1%) in the unit cell volume, which is in sharp contrast to the typical values (2–10%) for this phenomenon [51] and is due to the anisotropy of the structural rearrangement accompanying this spin transition. Raman spectroscopy measurements demonstrated that the sample is completely transformed to the LS state with increasing pressure to 2.87 GPa at room temperature.

The cooling of $[Fe(dpp)_2(NCS)_2]\cdot py$ from 275 to 150 K at atmospheric pressure leads to a reduction in the unit cell volume (by 2%) and a decrease in the unit cell parameter $b$ (by 3%), but the parameter $a$ increases (by 1%). Therefore, TEC of this compound in the $a$ direction is negative, and its magnitude, as emphasized by Shepherd *et al.*,[48] is comparable with the largest reported magnitudes of NTEs (from $-120$ to $-130\times10^6$ K$^{-1}$). The HS → $LS_T$ transition (the low-temperature low-spin phase) induced by cooling to $<$150 K leads to a decrease in the unit cell parameter $a$ by 3.5% and also to a significant increase in the parameter $b$ (by 13.9%).[48] In the authors opinion, the observed dynamics is associated with a change in the angle between the mean planes of the dpp ligands, which increases from 107.22(5)° under ambient conditions to 120.1(3)° at 2.48 GPa. On decompression, this angle decreases to 107.19(7)°, *i.e.*, to the initial value. The cooling of the crystal to 90 K leads to a decrease in the angle to 92.4(1)°. Consequently, the structure of the high-pressure low-spin phase ($LS_P$) differs from that of $LS_T$. Therefore, the detailed analysis of the pressure-induced [48] and temperature-induced [77] transformations of the complex $[Fe(dpp)_2(NCS)_2]py$ is necessary for an understanding of the effect of structural factors on the properties of the compound, such as the spin transition and negative linear compressibility.

Another pressure-induced effect is the stabilization of the high-spin state observed for the 2D polymer $[Fe(btr)_2(NCS)_2]\cdot H_2O$, where btr is 4,4′-bis(1,2,4-triazole).[78] The main pressure-induced changes in the magnetic properties of this compound are as follows: spin transitions both on heating and cooling are more continuous and are shifted to higher temperatures. The hysteresis loop width decreases, and the hysteresis completely disappears at ~1 GPa; simultaneously, the system shows the unexpected effect of pressure-induced stabilization of the high-spin state. On decompression, the hysteresis is restored, but a significant amount of the sample remains in the high-spin state at low temperatures; the relaxation to the initial level (~30%) takes ~175 h at room temperature.

The possibility of controlling the spin transition temperature by varying the external pressure was demonstrated for $Cs\{[Fe(3\text{-}CNpy)_2][Re(CN)_8]\}\cdot H_2O$, where 3-CNpy is 3-cyanopyridine.[79] The crystal structure of this compound consists of sheets formed by cyanide-bridged $Fe^{II}$ and $Re^{V}$ ions, which are linked by $Cs^+$ cations. The complex $Cs\{[Fe(3\text{-}CNpy)_2][Re(CN)_8]\}\cdot H_2O$ exhibited a two-step spin transition. Hysteresis loops were observed in both steps, which is indicative of a high cooperativity of the spin transition. Chorazy *et al.*[79] attributed this effect to the presence of two crystallographically independent units, {Fe1} and {Fe2}, in the structure, which form significantly different short interactions with interlayer $Cs^+$ ions. It should be noted that octacyanidometallates are quite often used as efficient building blocks in the synthesis of molecular nanomagnets. It was demonstrated that these compounds can act as magnetic coolers, spin-crossover materials, photomagnets, solvatomagnetic materials, including molecular magnetic sponges, luminescent and chiral magnets, pyroelectrics and ferroelectrics, ion conductors and electrochemical containers. For some octacyanometallate-based compounds, the pressure effect on the physicochemical properties was studied, and it was shown that the applied pressure can lead both to an increase in $T_c$ and the suppression of magnetic ordering due to the spin transition.[49, 80, 81] Studies of multifunctional magnetic materials, which combine several properties, for example, the spin transition and light sensitivity or conductivity, are of particular interest.

Examples of compounds, in which the multifunctionality is induced by an external pressure, are more rare. This phenomenon was observed in the polymer complex containing $Fe^{II}$ and $Nb^{IV}$ and exhibiting photomagnetic properties. The photomagnetism has attracted great attention since its discovery [82] because, as opposed to conventional magnets based on metals, their alloys or oxides, the spin state and magnetization of photomagnets are light-controlled. Most of the studied photomagnets belong to one of the following two classes:

— spin-crossover photomagnets;[83–85]
— charge transfer photomagnets.[86–88]

The former photomagnets exhibit light-induced excited spin state trapping (LIESST) phenomenon,[89] resulting in the switching between the LS and HS states of the metal ion. In the latter class of photomagnets, the electron transfer between two metal centres occurs.

The polymer $\{[Fe^{II}(Pz)_4]_2[Nb^{IV}(CN)_8]\cdot 4H_2O\}_n$ (Pz is pyrazole) and the isostructural manganese niobium complex do not exhibit photomagnetic behaviour at atmospheric pressure and do not display spin crossover phenomena.[49, 90] Under an applied pressure, the relative compression of the Fe–Nb complex is much higher compared to that of the related Mn–Nb complex, which does not have states of different spin multiplicity. The pressure-induced decrease in the unit cell volume and the Fe–N bond lengths is typical of compounds exhibiting spin crossover: the $Fe-N_{CN}$ and $Fe-N_{Pz}$ distance, which are 2.198(3) and 2.171(2) Å, respectively, at atmospheric pressure are decreased to 1.953(13) and 1.91(6) Å at 2.88 GPa. The compression is accompanied by piezochromism with a colour change from pink to dark blue under an applied pressure.[49]

At atmospheric pressure and low temperatures, the iron niobium complex displays ferrimagnetic behaviour. An increase in the pressure to 0.3–0.5 GPa does not cause significant changes in the magnetic properties of the compound but leads only to a lowering of the ordering tempe-

rature. The fraction of $Fe^{2+}$ ions in the LS state gradually increases with increasing pressure. At a pressure of $>0.5$ GPa, the character of magnetic ordering changes from ferrimagnetic to antiferromagnetic (spontaneous magnetization disappears). At a pressure of $>0.8$ GPa, the transition to the antiferromagnetic state gradually becomes blurred and disappears at 1.0 GPa, because the compound shows paramagnetic behaviour in the whole measurement range. High-pressure photomagnetic measurements in the range of 0.6–1.0 GPa demonstrated that the magnetization increased immediately after the light irradiation of the sample. Thus, at 0.6 GPa and 2 K in a magnetic field of 100 Oe, the magnetization increased by a factor of 2.7 after 20 min. At a pressure of $>1$ GPa, the photomagnetic effect was completely suppressed. At a pressure of about 0.6–1.0 GPa, the light-induced long-range magnetic order in the iron–niobium complex was restored through the switching of $Fe^{2+}$ ions to the high-spin state due to the LIESST effect. This resulted in the restoration of magnetic exchange through the $-Nb^{IV}-CN-Fe^{II}-$ pathway, giving rise to the magnetic ordering of the photoinduced phase.

Therefore, investigations of the pressure effect on the crystal structures of compounds exhibiting spin transition are important for an understanding of the effect of the structural factors on the properties of the compound. These studies are complicated by the polymorphism of compounds. Nevertheless, it was established with confidence that the pressure increase not only leads to a change in $T_c$ but also can stabilize the high-spin state and cause the piezochromism and photomagnetism.

## 3. Pressure-induced valence tautomerism

In valence tautomeric complexes, a change in the temperature and(or) pressure can induce the intramolecular electron transfer from the ligand to the metal centre or backward.[91–95] In some cases, the valence tautomerism is considered as the sum of the following two sequential processes: the spin transition at the metal centre and the subsequent intramolecular electron transfer between the metal ion and the redox-active ligand.[96] The pressure-induced valence tautomerism was first reported in 1996.[93] The solid-state conversion of the high-spin complex $[Co^{II}(3,5\text{-}SQ)_2(phen)]\cdot x\,Solv$ (Solv is toluene; $x = 0$, 1) to the low-spin complex $[Co^{III}(3,5\text{-}SQ)(3,5\text{-}Cat)(phen)]\cdot x\,Solv$, where 3,5-SQ and 3,5-Cat are the semiquinonate and catecholate forms, respectively, of 3,5-di(*tert*-butyl)-*o*-benzoquinone, was studied by X-ray spectroscopy methods, EXAFS and XANES (X-ray absorption near edge structure). It was found that the cooling of $[Co(3,5\text{-}SQ)_2(phen)]\cdot Solv$ containing the high-spin $Co^{II}$ cation below 215 K leads to the intramolecular electron redistribution, giving rise to the low-spin $Co^{III}$ complex. At room temperature, the Co–O and Co–N bond lengths are $2.08\pm0.02$ and $2.13\pm0.02$ Å, respectively; at 200 K these distances are much shorter ($1.91\pm0.02$ and $1.93\pm0.02$ Å). The unsolvated complex is not transformed into its electromer‡ down to 2 K. However, under an applied pressure, the valence tautomerism is observed in both complexes. In $[Co(3,5\text{-}SQ)_2(phen)]\cdot Solv$, the transition occurs at 0.075–0.700 GPa, whereas a higher pressure (0.10–2.5 GPa) is required for the unsolvated complex $[Co(3,5\text{-}SQ)_2(phen)]$. Both temperature- and pressure-induced tautomeric transformations are reversible.

High-pressure magnetochemical measurements of [Co(L)(diox)]X, where L is D,L-5,7,7,12,14,14-hexamenthyl-1,4,8,11-tetraazacyclotetradecane, diox is 9,10-dioxophenanthrene and $X = PF_6^-$, $BPh_4^-$, $I^-$, demonstrated that the valence tautomeric transition temperature depends on the nature of the outer-sphere X anion.[94] Using a salt with $PF_6^-$, it was shown that the transition temperature increases with increasing pressure, and this compound is actually diamagnetic at 0.74 GPa even at room temperature.

The study of the crystal structure of the trinuclear dioxolene complex $[Co_3(3,5\text{-}SQ)_2(Bu^tCO_2)_4(NEt_3)_2]$ in the temperature range of 20–200 K revealed no significant changes. This is indicative of the absence of intramolecular electron transfer between the ligand and the metal centre and is consistent with the results of magnetic susceptibility measurements, which confirmed the absence of valence tautomerism.[97] The study of the crystal structure at a pressure of 2.5 GPa demonstrated that its response depends on the rate of pressure increase. When the pressure was gradually increased to 2.6 GPa, the structure of the compound remained almost unchanged. By contrast, a sharp increase in the pressure to 2 GPa caused a structural phase transition. In the resulting high-pressure phase, the symmetry was unchanged, while the unit cell volume was doubled, the coordination mode of one bridging $Bu^tCO_2$ ligand in one crystallographically independent molecule changed from bidentate bridging to bidentate chelating bridging (Fig. 1), whereas another molecule remained unchanged. It is worth noting that the phase transition has no effect on the spin and charge states of the metal ion and the ligands.

The study of the pressure effect on the valence tautomerism in the binuclear complexes $[\{Co(tpa)\}_2(dhbq)](PF_6)_3$ and $[\{Co(dpqa)\}_2(dhbq)](PF_6)_3$, where tpa is tris(2-pyridylmethyl)amine, dpqa is bis(2-pyridylmethyl)-*N*-(quinolin-2-ylmethyl)amine and dhbq is deprotonated 2,5-dihydroxy-*p*-benzoquinone, demonstrated that the temperature dependence of magnetic susceptibility [$\chi T(T)$] is shifted to the low-temperature region with increasing pressure to $\sim0.13$ GPa, which is opposite to the effects observed in the complexes studied previously.[91] A further increase in the pressure is accompanied by the shift of the $\chi T(T)$ plot towards higher temperatures. The authors attributed these effects to the fact that the transition occurs through a two-step process, involving the spin transition and the intramolecular electron transfer, and assumed that the pressure affects the spin transition step in the same way as in other spin-crossover complexes.

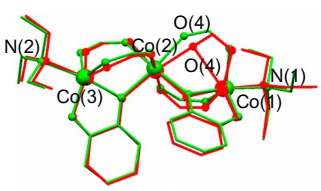


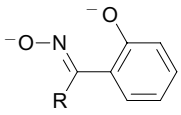

**Figure 1.** Change in the coordination mode of the O(4) atom of the bridging ligand accompanying the phase transition (225 K and $10^{-4}$ GPa, given in green) → (295 K and 1.35 GPa, given in red). The Figure was prepared by the authors using original data from the study.[97]

‡ From our point of view, the terms 'valence tautomers' and 'electromers' are synonyms. Historically, the term 'valence tautomers' was referred to a type of isomerism. In recent years, the term 'electromers' has been increasingly used as applied to coordination compounds, particularly to metal complexes with dioxolene ligands.

## 4. Single-molecule magnets

High-pressure experiments with single-molecule magnets are performed with the aim to obtain structure–property relationships in order to develop efficient approaches to the design of such magnets.[98,99] The study of the structure and magnetic properties of $[Mn_6O_2(Rsao)_6(R'CO_2)_2(L)_{4-6}]$, where $Rsao^{2-}$ is the dianion of R-substituted salicylaldoxime (structure **1**), demonstrated that the spin $S$ of the ground state of the complex can be changed from 4 to 12 in a stepwise manner by varying the substituents R and R′, thereby increasing the energy barrier for magnetization reorientation.[100] In the authors opinion, the change from antiferromagnetic to ferromagnetic exchange is associated with the Mn–N–O–Mn torsion angle value. Thus, the angles of $>31^\circ$ and $<31^\circ$ correspond to the ferromagnetic and antiferromagnetic exchange, respectively.

**Structure 1**




R = H, Me, Et  $Rsao^{2-}$, **1**

The high-pressure study of $[Mn_6O_2(Etsao)_6(O_2CPhMe_2)_2(EtOH)_6]$ and $[Mn_6O_2(Etsao)_6(O_2C\text{-naphth})_2(EtOH)_4(H_2O)_2]$, where $O_2C$-naphth is the naphtholate anion, (Fig. 2) made it possible to find qualitative correlations between the pressure-induced changes in the structure and magnetic properties of these compounds.[101] Out-of-phase magnetic susceptibility and hysteresis loop measurements demonstrated a significant decrease in the energy barrier for magnetization reversal and a weakening of the magnetic exchange between the metal centres. Besides, it was shown that an increase in the external pressure can give rise to the same effects as those observed upon chemical modification of the polymetallic core of the molecule.

The study of the trinuclear manganese(II,III) compound $[Mn_3(Hcht)_2(bipy)_4](ClO_4)_3 \cdot Et_2O \cdot 2\,MeCN$, where $H_3cht$ is *cis*,*cis*-cyclohexane-1,3,5-triol, (Fig. 3) demonstrated[102] a pressure-induced change in its composition. Thus, the elimination of solvent molecules from the solid phase was observed even at a minimum pressure of 0.16 GPa used in this work. This is a rare case of the external pressure-induced desolvation. The ejection of the solvent molecules leaves voids in the crystal, which are then progressively reduced with higher pressure (the volume of the voids is ~9% of the unit cell volume at 0.16 GPa and ~5.5% at 1.25 GPa). Most geometric parameters of the polymetallic core remain almost unchanged with increasing pressure. For this reason, the variation in the pressure has a slight effect on the magnetic behaviour of $[Mn_3(Hcht)_2(bipy)_4](ClO_4)_3 \cdot Et_2O \cdot 2\,MeCN$ and structurally similar compounds.[103–105]

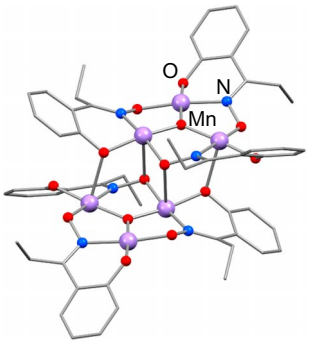



**Figure 2.** Structure of the $\{Mn_6O_2(Etsao)_6\}$ unit. The Figure was prepared by the authors using original data from the study.[100]

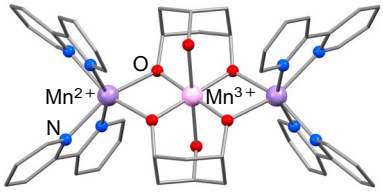



**Figure 3.** Structure of the complex cation $[Mn_3(Hcht)_2(bpy)_4]^{3+}$. The Figure was prepared by the authors using original data from the study.[102]

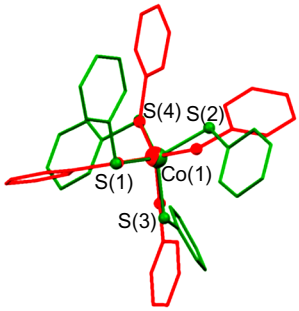



**Figure 4.** Structure of the $[Co(SPh)_4]^{2-}$ anion at $10^{-4}$ GPa (given in green) and 9.2 GPa (given in red). The Figure was prepared by the authors using original data from the study.[18]

The mononuclear single-molecule magnet $(PPh_4)_2[Co(SPh)_4]$ (Fig. 4) showed slow magnetization relaxation.[18] An increase in the pressure leads to a gradual decrease in the volume of intermolecular voids (regions with low electron density)[18] and a change in the geometry of the molecule. The shortening of the Co–S bonds and changes in the S(4)–Co–S(2) and S1–Co–S(3) angles have the most significant effect on the magnetic properties. The *ab initio* calculations at the NEVPT2 level of theory demonstrated changes in the energy difference between the $d_{x^2-y^2}$ and $d_{xy}$ orbitals. The splitting of d orbitals in general decreases with pressure. The changes in the S–Co–S angles, which are significantly smaller than the ideal tetrahedral angle (109.5°) even at ambient pressure, have a decisive effect on the parameter characterizing magnetic anisotropy ($D$). At a pressure of >1 GPa, these angles decrease by ~5°. This change is sufficient to provide nearly a doubling of the parameter $D$ due to the relative stabilization of the energy of the $d_{xy}$ orbital and, consequently, a decrease in the energy difference between the $d_{x^2-y^2}$ and $d_{xy}$ orbitals. Apart from the investigation of the effects of the S–Co–S angles and Co–S bond lengths, the theoretical study of the influence of the second coordination sphere was performed, which showed the importance of the rotation of phenyl rings. The authors developed an approach to the rational design of single-molecule magnets with a higher anisotropy based on bidentate sulfur-containing ligands, which provide the right S–Co–S angles.

## 5. Organic paramagnets

Organic ferromagnets have a number of advantages over conventional magnetic materials: they are light-weight, do not conduct electricity, are transparent and can be synthesized at ambient temperature. A detailed analysis of magnetic structural correlations using quantum chemical calculations are required in order to elucidate the mechanisms of interactions in organic ferromagnets. As men-

tioned above, it is necessary to take into account that even a small variation in the composition can often lead to the formation of another crystal packing and, correspondingly, to another magnetic behaviour of the compound. Therefore, investigations of structural transformations during a gradual change in the pressure provide valuable data on magnetic structural correlations.

Studies of pressure-induced changes in the magnetic ordering temperature or exchange interactions in crystals of organic radicals, started in the late 1980s, are scarce, and the data on changes in the crystal structures are almost lacking.[106–118] The studies, [119–121] in which these data were reported [*e.g.*, for a radical anion salt with an organic cation and the bis(dithiazolyl) radical, forming dimers in the solid state], are rare. However, the data on the high-pressure magnetic properties of the compounds are absent even in these publications.

Semiquinone, thiazolyl, verdazyl and nitroxide radicals often form tightly connected stacks of dimers with interplanar distances within dimeric units of about 3.5 Å.[122–125] Taking into account this arrangement, it can be suggested that there are rather strong exchange interactions in radical pairs, which can lead to spin pairing in these pairs and give rise to diamagnetism with increasing pressure.

High-pressure studies of the magnetic properties of the galvinoxyl (Galv, structure **2**) [126] and fluorinated nitroxide $F_5$PNN (structure **3**) radicals [108] demonstrated that the structural changes in both compounds induced by lowering temperature can be suppressed with pressure. The phase transition of Galv to the diamagnetic state, observed at ambient pressure, is almost completely suppressed at 0.7 GPa, and the magnetism of the radical is retained down to low temperatures. The magnetic behaviour of $F_5$PNN at room temperature is described by a model of a uniform antiferromagnetic chain, whereas the low-temperature magnetism is rationally described in terms of an alternating antiferromagnetic chain. At a pressure of 0.5 GPa, the low-temperature magnetism follows a model of a uniform antiferromagnetic chain, which confirms the retention of the crystal structure throughout the temperature range.

Studies of the crystal structures and conductivity of three oxobenzylbis(dithiazolyl) radicals O-TDAZ-R (R = H, F, Ph; structures **4a–c**) at a pressure in the range of 0–15 GPa demonstrated that O-TDAZ-H undergoes two structural phase transitions, whereas no phase transitions are observed for O-TDAZ-R (R = F, Ph).[117] Structural changes in all O-TDAZ-R radicals are associated with displacements of the molecules in the layer (Fig. 5) and a reduction of the distances between the parallel molecules of the adjacent layers. Thus, the distances in O-TDAZ-F decrease from 3.153 Å at ambient pressure [127] to 2.787 Å at 8.9 GPa.[117] A decrease in the temperature leads to the ordering of all three radicals as weak antiferromagnets, but this effect disappears at a pressure of ~1.5 GPa. At room temperature, the electrical conductivity rapidly increases with pressure. For O-TDAZ-F, a wide range ($T$ = 5–300 K) of the quasiquadratic temperature dependence of resistivity was found at 6.2 GPa.

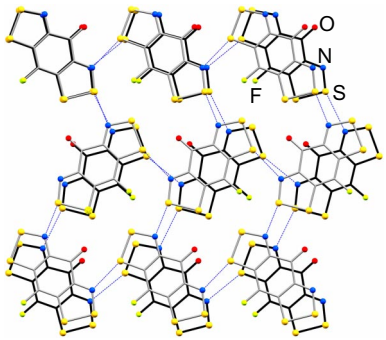
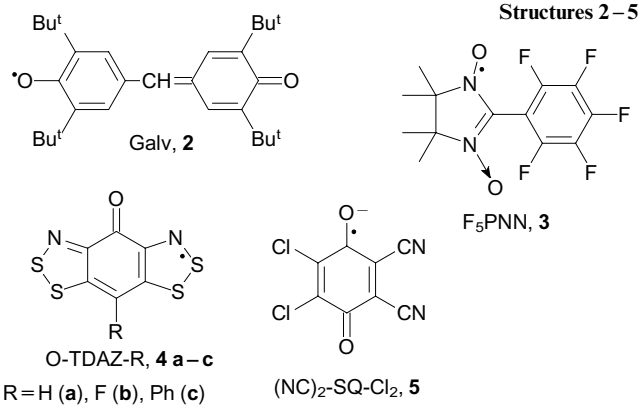



**Figure 5.** Displacement of O-TDAZ-F molecules in the layer with increasing pressure from atmospheric pressure (shown in black) to 8.9 GPa (shown in gray). The shortest contacts are indicated by dashed lines. The Figure was prepared by the authors using original data from the study.[109]

Two substituted bis(dithiazolyl) radicals btz-Et-F and btz-Me-F crystallize as two polymorphs. The crystals of the α-phase contain radicals, whereas the crystals of the β-phase consist of dimers, in which the paramagnetic centres quench each other through the formation of the four-centre six-electron S···S–S···S bond (Fig. 6). The application of an external pressure of ~0.8 GPa, the light irradiation ($\lambda$ = 650 nm) at low temperature or the heating to 380 K at ambient pressure caused the dissociation of β-btz-Et-F dimers to form a pair of radicals.[128] This was confirmed by the single-crystal X-ray diffraction study of a sample after irradiation, magnetochemical measurements at ambient pressure and high-pressure powder X-ray diffraction data. On the contrary, the β-btz-Me-F dimers do not decompose at temperatures up to 400 K and at pressures up to 8 GPa, and only the irradiation at low temperature can cause their dissociation.[120, 121]

In the structure of the 4-cyano-*N*-methylpyridinium salt of the 5,6-dichloro-2,3-dicyanosemiquinone radical anion, the $(NC)_2$-SQ-$(Cl)_2$ radical anions (structure **5**) are packed in stacks, which contain dimers with interplanar distances of 2.922 Å and the distances between the adjacent dimers of 3.488 Å (the distances between the {C6} centroids of the radical anions are 3.533 and 4.051 Å).[119] The study of temperature-induced transformations of this structure

**Structures 2–5**



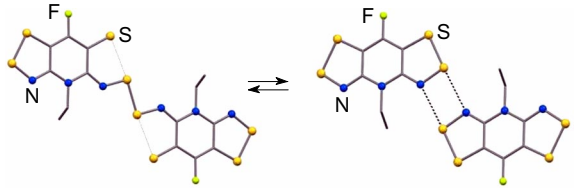




**Figure 6.** Dimers linked by a S···S–S···S σ-bond in the β-phase of btz-R (R = Me, Et) (on the left) and a pair of the radicals generated from β-btz-Et under a pressure of 0.98 GPa; the short N–S contacts are indicated by dashed lines; hydrogen atoms are omitted for clarity. The Figure was prepared by the authors using original data from the study.[128]

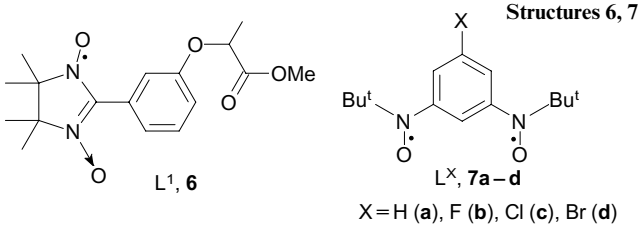
revealed a phase transition in the temperature range from 210 to 240 K, which was detected from the inflection points in the temperature dependences of the unit cell parameters (*b* and *c*) and the unit cell volume. It was demonstrated that this transition is accompanied by the expansion of the structure along the stacks. The application of a pressure of up to 2.00 GPa leads to a rapid decrease in the distance between the dimers, the interplanar distances in the dimers being varied in a much narrow range. At 2.55 GPa, these distances are nearly equal. At the maximum pressure of 6 GPa achieved in this study, the interplanar distance in the dimer is nearly equal to that observed under ambient conditions (~2.93 Å), whereas the spacing between the dimers decreases by more than 0.7 Å and reaches 2.756(5) Å, which is almost equal to the theoretically predicted shortest interplanar distance for this arrangement of radicals. In the studies,[129, 130] the authors mentioned the following: if the interaction between radicals in the dimers is considered as delocalized two-electron multicentre bonding with a significant covalent contribution, this contribution significantly increases with pressure, which is consistent with the results of density functional theory (DFT) calculations.

## 6. Metal complexes with organic paramagnets. Breathing crystals

Metal complexes with semiquinonates, nitroxides, verdazyls and other organic radicals are poorly studied in relation to the response of the crystal structure and magnetic properties to the applied external pressure. One of such compounds is the chain polymeric complex of $Rh^{I}$ semiquinonate with the 3,6-di(*tert*-butyl)-4,5-dimethoxy-1,2-benzosemiquinone radical anion [Rh(3,6-DBSQ-4,5-$(MeO)_2$)$(CO)_2$],[131] exhibiting bistability of magnetic and conductive properties in the temperature range of 228–207 K. The bistability results from the thermal hysteresis of the phase transition, which is associated with exchange interactions between semiquinonate anions of the adjacent chains. Magnetic interactions in the chain drastically change from strongly ferromagnetic in the low-temperature phase to antiferromagnetic in the room-temperature phase. In addition, this compound exhibits long-range antiferromagnetic ordering between ferromagnetic chains and spontaneous magnetization at a Néel temperature ($T_N$) of 14.2 K. The low-temperature phase can be stabilized up to room temperature by the application of a relatively low pressure (0.14 GPa), which allows the control of physical parameters through external stimuli.[132]

Metal complexes with nitroxide radicals (*e.g.*, $L^1$, structure **6**) is another representative group of magnetically active compounds, many of which display unusual magnetic properties. It is worth noting that the effect of an external pressure on the magnetic properties and crystal structure of

**Structures 6, 7**



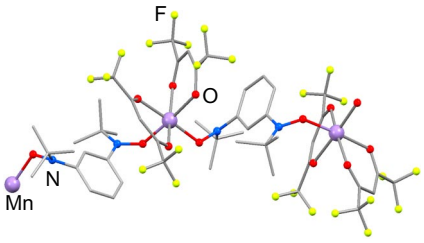




**Figure 7.** Fragment of the $[Mn(hfac)_2L^H]$ chain. Hydrogen atoms are omitted for clarity. The Figure was prepared by the authors using original data from the study.[135]

metal complexes with nitroxides remained almost unknown until recently, although the first studies were published back in the 1990s.[133–137]

It was demonstrated that the polymer chain complexes $[Mn(hfac)_2L^X]$, generated in the reaction of divalent manganese hexafluoroacetylacetonate $Mn(hfac)_2$ with 1,3-bis(*N*-*tert*-butylaminoxyl)benzene and its 5-halogenated derivatives $L^X$ (X = H, F, Cl, Br; structures **7a–d**), are molecular magnetic materials (Fig. 7).[134, 135] Due to specific features of the mutual arrangement of the chains in the solid state of these complexes, $[Mn(hfac)_2L^H]$ and $[Mn(hfac)_2L^F]$ behave as metamagnets with weak interchain antiferromagnetic interactions in thermomagnetic studies under ambient pressure, whereas $[Mn(hfac)_2L^{Cl}]$ and $[Mn(hfac)_2L^{Br}]$ are ferrimagnets with weak interchain ferromagnetic interactions. For metamagnets, an increase in the hydrostatic pressure brings about the enhancement of interchain antiferromagnetic interactions and an increase in $T_N$, whereas the ferrimagnet $[Mn(hfac)_2L^{Cl}]$ is transformed into a metamagnet under an applied pressure.

At low temperatures, the ferromagnetic ordering temperature of the coordination polymer $Mn(hfac)_2$ with optically active nitronyl nitroxide radical **6** significantly increases with increasing pressure to 0.10 GPa.[137]

Divalent copper hexafluoroacetylacetonate complexes with nitroxide radicals belong to breathing crystals, which can undergo reversible magnetic structural phase transitions without degradation. These crystals were called breathing because of a significant change in the unit cell volume of these crystals, which reaches 10–13% after repeated cooling–heating cycles.[21] Breathing crystals may exhibit temperature dependence of the effective magnetic moment ($\mu_{eff}$) similar to that observed for iron complexes showing spin transition. The classical spin crossover is impossible for the $Cu^{2+}$ ion in complexes with diamagnetic ligands. However, the coordination of radical centres of organic paramagnetic ligands affords heterospin exchange clusters; in the case under consideration, clusters containing two $\{>N-O^{\bullet}-Cu^{2+}\}$ or three $\{>N-O^{\bullet}-Cu^{2+}-O^{\bullet}-N<\}$ paramagnetic centres (Fig. 8). In this case, a change in the $\mu_{eff}$ value is related to a change in the total spin of the heterospin cluster.

Since $Cu^{II}$ is a Jahn–Teller ion typically having an elongated octahedral coordination, the radical can be coordinated either axially with $Cu-O_{NO}$ distances of about 2.4–2.5 Å or equatorially ($Cu-O_{NO}$, *ca.* 1.9 Å).[139] The exchange in the heterospin cluster significantly depends on the coordination mode of the radical. Thus, weak ferromagnetic exchange corresponds to the axial coordination; strong antiferromagnetic exchange, to equatorial coordination.[21, 140] The phase transition in such complexes is associated with a change in the coordination geometry of the $Cu^{II}$ ion, manifested in the reorientation of the Jahn-Teller elongation, which is accompanied by a change in $\mu_{eff}$ due to

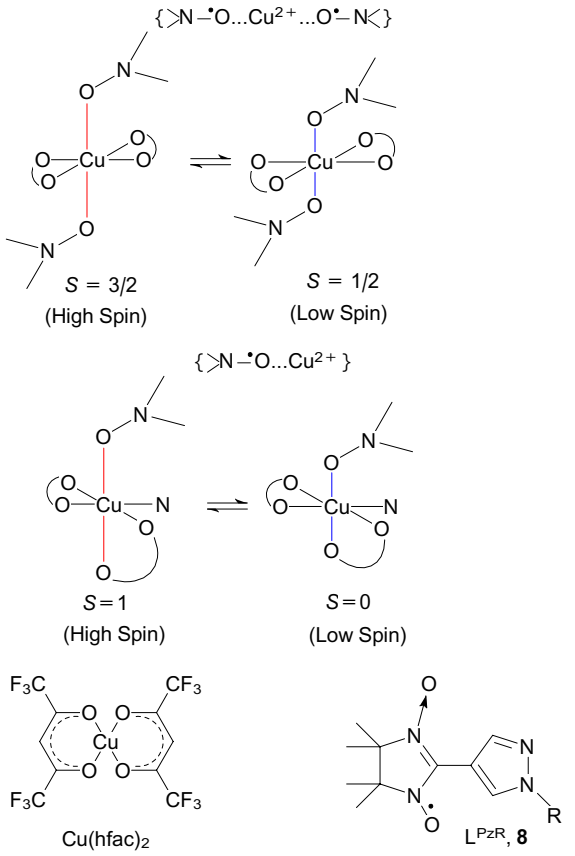


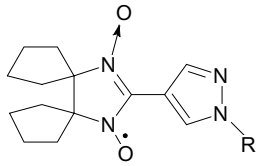

**Figure 8.** Exchange clusters in the complexes $Cu(hfac)_2$ with nitroxide radicals $L^R$ and their ($T$,$P$)-induced structural rearrangements.

switching of the character of copper-radical exchange interaction. Such transitions can be induced by temperature at ambient pressure or by irradiation. Therefore, the LIESST effect accompanied by thermal hysteresis and(or) thermochromism can appear in these complexes, like in classical spin-crossover compounds.[11, 21, 141–144]

As mentioned above, breathing crystals can experience a temperature-induced reversible phase transition without degradation. Hence, it was suggested that transitions can be caused by the applied external hydrostatic pressure. In the case of a large change in the unit cell volume, these compounds can be highly sensitive to the external pressure. Like in classical spin-crossover compounds, the pressure effect on the magneto-structural transitions in divalent copper complexes with L leads, in the first approximation, to a change in the temperature of this transition due to a change in the energy difference between the HS and LS states by a value corresponding to the work against the external pressure during the phase transition. Generally, the low-spin state has a higher density and, therefore, this state is stabilized by the applied pressure. However, apart from the shift of $T_c$, there are also non-trivial effects associated with qualitative difference between the pressure- and temperature-induced structural dynamics. Thus, the magnetic transition in the compound $[Cu(hfac)_2]_3(L^{Br})_2$ with a molecular structure was completely suppressed at a pressure of ~0.6 GPa, and the complex was in the high-temperature phase in the whole temperature range under study.[133, 136] Moreover, it was found that even a simple immersion of this complex into a pressure transmitting medium without additional compression led to a significant change in the magnetic properties compared to the properties of the complex at ambient pressure. However the high-pressure structure of the complex was not determined. Therefore, it is difficult to explain the factors responsible for this pressure effect on magneto-structural transitions.

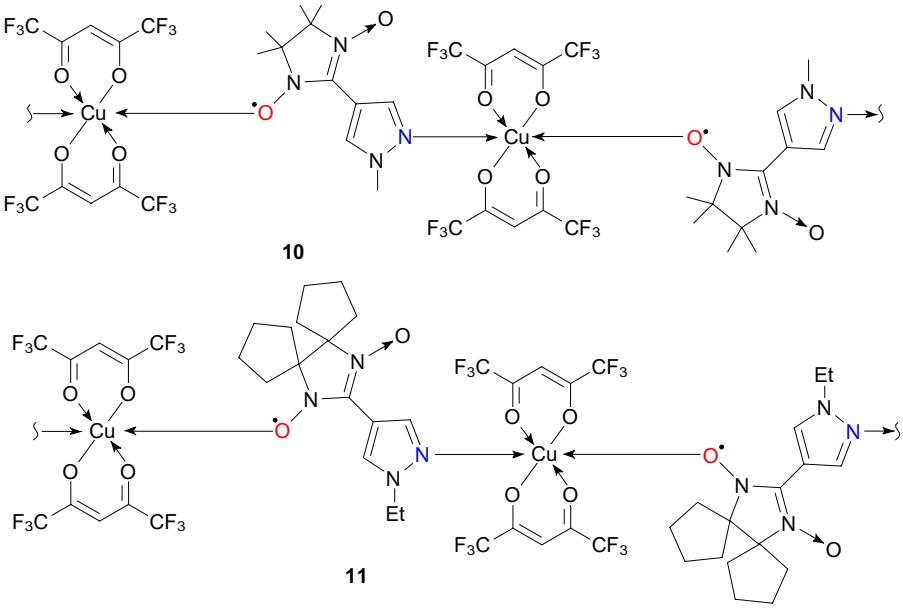
High-pressure X-ray diffraction studies are obviously desirable but they are not always possible. A significant bottleneck is the crystal destruction at high pressure. As an example let us refer to the complexes $Cu(hfac)_2$ with pyrazolyl-substituted nitronyl nitroxides $L^{PzR}$ (structure **8**) and $L^{*PzR}$ (structure **9**), the magnetic properties of which were studied at a pressure of up to 1 GPa in the temperature range of 5–300 K.[143, 145–147] These compounds have a polymer chain structure and exhibit reversible magneto-structural transitions at ambient pressure, resulting in the change in the character of exchange interactions between the paramagnetic centres (the $Cu^{II}$ ion and the radical). In the structure, this is manifested in the change in the distance between the copper atom and the nitroxide oxygen atom and in the change in the direction of the Jahn–Teller elongation axis in the square-bipyramidal environment of $Cu^{II}$ (see Fig. 8).[21, 148, 149]

**Structure 9**




The crystals of the complex $[Cu(hfac)_2L^{PzMe}]$-I with a head-to-tail polymer chain motif (structure **10**) undergo a complex sequence of temperature-induced transformations at ambient pressure. On cooling, the initial monoclinic phase $[Cu(hfac)_2L^{PzMe}]$-I-m, in which all coordination units $\{CuO_5N\}$ are identical, is transformed into the triclinic phase $[Cu(hfac)_2L^{PzMe}]$-I-t1 in the temperature range of 235–245 K. Due to the symmetry lowering, the asymmetric unit of the structure is doubled, and the chains consist of alternating $\{CuO_5N\}$-1 and $\{CuO_5N\}$-2 units with slightly different geometry. Upon further cooling, the phase t1 is transformed into $[Cu(hfac)_2L^{PzMe}]$-I-t2 at 145–150 K and it remains intact down to 2 K. Upon subsequent heating, the polymorph t2 is transformed into the polymorph t1 at a temperature above 150 K and is then transformed into the initial monoclinic phase at 350 K. The transitions between the triclinic and monoclinic phases are purely structural, *i.e.*, they are related to symmetry changes, and slightly affect the $Cu-O_{NO}$ bond length. Hence, these transitions are almost not reflected in the magnetic properties. Meanwhile, the t1 → t2 or t2 → t1 transition without symmetry changes leads to the reorientation of the Jahn–Teller axis in half of the $\{CuO_5N\}$ coordination units. At 145 K in half of the $\{CuO_5N\}$-1 coordination units, the $Cu-O_{NO}$ distance significantly decreases [from 2.507(7) Å at room temperature to 1.977(8) Å at 140 K]. In these coordination units, a concomitant increase in the distance is observed from the copper atom to two $O_{hfac}$ atoms [from ~1.9 Å (295 K) to 2.288(7) and 2.250(8) Å (140 K), respectively]. As a result, the character of exchange interactions in this half of exchange clusters $\{Cu-O^{\bullet}-N<\}$ changes from ferromagnetic to strong antiferromagnetic, resulting in a

**Structures 10, 11**




drastic decrease in $\mu_{eff}$. It is worth noting that the complex [Cu(hfac)$_2$L$^{PzMe}$]-I shows thermochromic behaviour with a colour change from blue to dark green on cooling.

Unfortunately, single crystals of [Cu(hfac)$_2$L$^{PzMe}$]-I underwent degradation even under a small external pressure (~0.07 GPa), which made it impossible to obtain data on pressure-induced structural transformations of this complex. Thermomagnetic studies of [Cu(hfac)$_2$L$^{PzMe}$]-I showed that the temperature of the t1 → t2 transition increases by ~100 K at an applied pressure of 0.04 GPa.[145] At a pressure of 0.32 GPa, half of exchange clusters exist in a strongly coupled state, which possesses antiferromagnetic exchange interaction in the {Cu—O$^{\bullet}$—N<} cluster, already at 350 K. The study in the pressure range of 0.03–0.15 GPa demonstrated that the sensitivity of the transition temperature of this compound to the pressure is $590 \pm 100$ K GPa$^{-1}$, which is significantly higher compared to most of the studied iron complexes exhibiting spin crossover (~146–220 K GPa$^{-1}$, see above).

The solid state of the polymer chain complex [Cu(hfac)$_2$L$^{*PzEt}$] with the same polymer chain motif (see structures **9** and **11**) undergoes an abrupt magneto-structural transitions at ambient pressure in the temperature range of 120–130 K. In all {CuO$_5$N} coordination units, the direction of the Jahn–Teller axis changes from $N_{Pz}$—Cu—$O_{NO}$ to $O_{hfac}$—Cu—$O_{hfac}$ and the Cu—$O_{NO}$ bond length decreases by 0.433 Å, which is accompanied by the appearance of the strong antiferromagnetic exchange interaction between the unpaired electrons of the copper ions and the radical. The resulting complex displays diamagnetic behaviour. As in the case of [Cu(hfac)$_2$L$^{PzMe}$]-I, the application of the hydrostatic pressure leads to an increase in the phase transition temperature of [Cu(hfac)$_2$L$^{*PzEt}$]; a nearly linear change in the $T_c$ value is observed in the pressure range of 0.08–0.48 GPa. The pressure-induced shift of $T_c$ for this compound was $290 \pm 15$ K GPa$^{-1}$. All the above pressure-induced changes in the magnetic properties are completely reversible. Let us also mention the piezochromism of [Cu(hfac)$_2$L$^{*PzEt}$]; thus, an increase in the pressure leads to a change in the colour of a powdered sample from blue to red.[143]

The crystals of [Cu(hfac)$_2$L$^{*PzEt}$] proved to be more elastic compared to [Cu(hfac)$_2$L$^{PzMe}$]-I, and the applied pressure did not lead to their degradation. This made it possible to reveal the changes in the crystal structure. It was demonstrate that the Cu—$O_{NO}$ and Cu—$N_{Pz}$ bond lengths in the coordination units decrease by at most 0.06 Å with increasing pressure from $10^{-4}$ to 0.28 GPa, whereas these distances decrease by 0.29 and 0.15 Å and reach 2.10(2) and 2.11(3) Å, respectively, in the range of 0.28–0.45 GPa. In general, the temperature- and pressure-induced structural transformations have a similar character (Fig. 9).

Apart from the head-to-tail polymer chain phase [Cu(hfac)$_2$L$^{PzMe}$]-I considered above, there is the polymorph [Cu(hfac)$_2$L$^{PzMe}$]-II with a head-to-head polymer chain motif.[146] The crystal structures of the complexes Cu(hfac)$_2$ with nitronyl nitroxide radicals L$^{PzR}$, where R = Et, All ($CH_2CH{=}CH_2$), are also formed by polymer chains with this motif.[148, 150, 151] Structure **12** illustrates the structure of such chains. They consist of alternating {CuO$_6$} coordination units, which are three-spin exchange clusters {>N—$^{\bullet}$O—Cu$^{II}$—O$^{\bullet}$—N<}, and the {CuO$_4$N$_2$} units. In all complexes [Cu(hfac)$_2$L$^{PzR}$] with this polymer chain motif, the Cu—$O_{NO}$ distances in the {CuO$_6$} coordination units are shorter [2.243(3)–2.336(1) Å] than the Cu—$N_{Pz}$ distances in the {CuO$_4$N$_2$} coordination units [2.373(3)–2.557(2) Å].

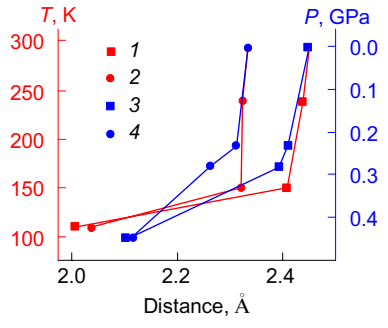
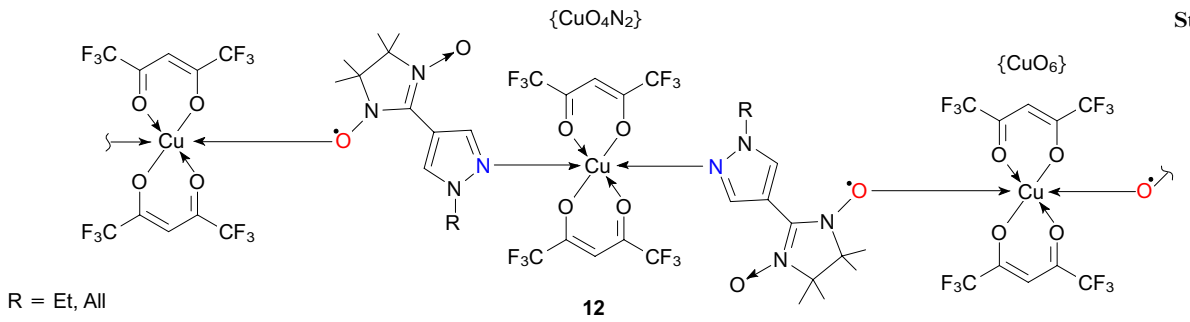



**Figure 9.** Plots of the Cu—$O_{NO}$ (*1*, *3*) and Cu—$N_{Pz}$ (*2*, *4*) distances *versus* the temperature at $P = 10^{-4}$ GPa (*1*, *2*) and *versus* the pressure at $T = 300$ K (*3*, *4*) for [Cu(hfac)$_2$L$^{*PzEt}$]. The Figure was prepared by the authors using original data from the study.[143]

**Structure 12**




The chains in this series of complexes adopt the same structural motif; however, their packing modes in the crystal structures are different (Fig. 10 *a*,*b*). As a result, the temperature-induced structural transformations have a different character (Fig. 10 *c*). In the structure of $[Cu(hfac)_2L^{PzMe}]$-II, all chains are parallel, whereas the parallel chains in the isostructural complexes with $L^{PzEt}$ and $L^{PzAll}$ form alternating layers rotated with respect to each other by an angle of ~45°. Despite the fact that these complexes differ only by a slight modification of the nitroxide radical, their magnetic properties at ambient pressure are remarkably different (see Fig. 10 *c*). Thus, a gradual stepwise decrease in the $\mu_{eff}$ value occurs on cooling of $[Cu(hfac)_2L^{PzMe}]$-II, whereas the initial gradual decrease in $\mu_{eff}$ of $[Cu(hfac)_2L^{PzEt}]$ and $[Cu(hfac)_2L^{PzAll}]$ (Ref. 147) as the temperature decreases from 300 to ~220 K for the former complex and to ~130 K for the latter one is followed by an increase in this parameter upon further cooling.

For $[Cu(hfac)_2L^{PzMe}]$-II, the $Cu-O_{NO}$ distance in the $\{CuO_6\}$ coordination units decreases stepwise by 0.336 Å as the temperature decreases from 300 to 30 K (Fig. 11 *a*). Simultaneously, the Cu–O bonds along the $O_{hfac}-Cu-O_{hfac}$ axis are elongated by a comparable value. Therefore, the cooling leads to a change in the direction of the elongated axis in the bipyramid of $Cu^{II}$.

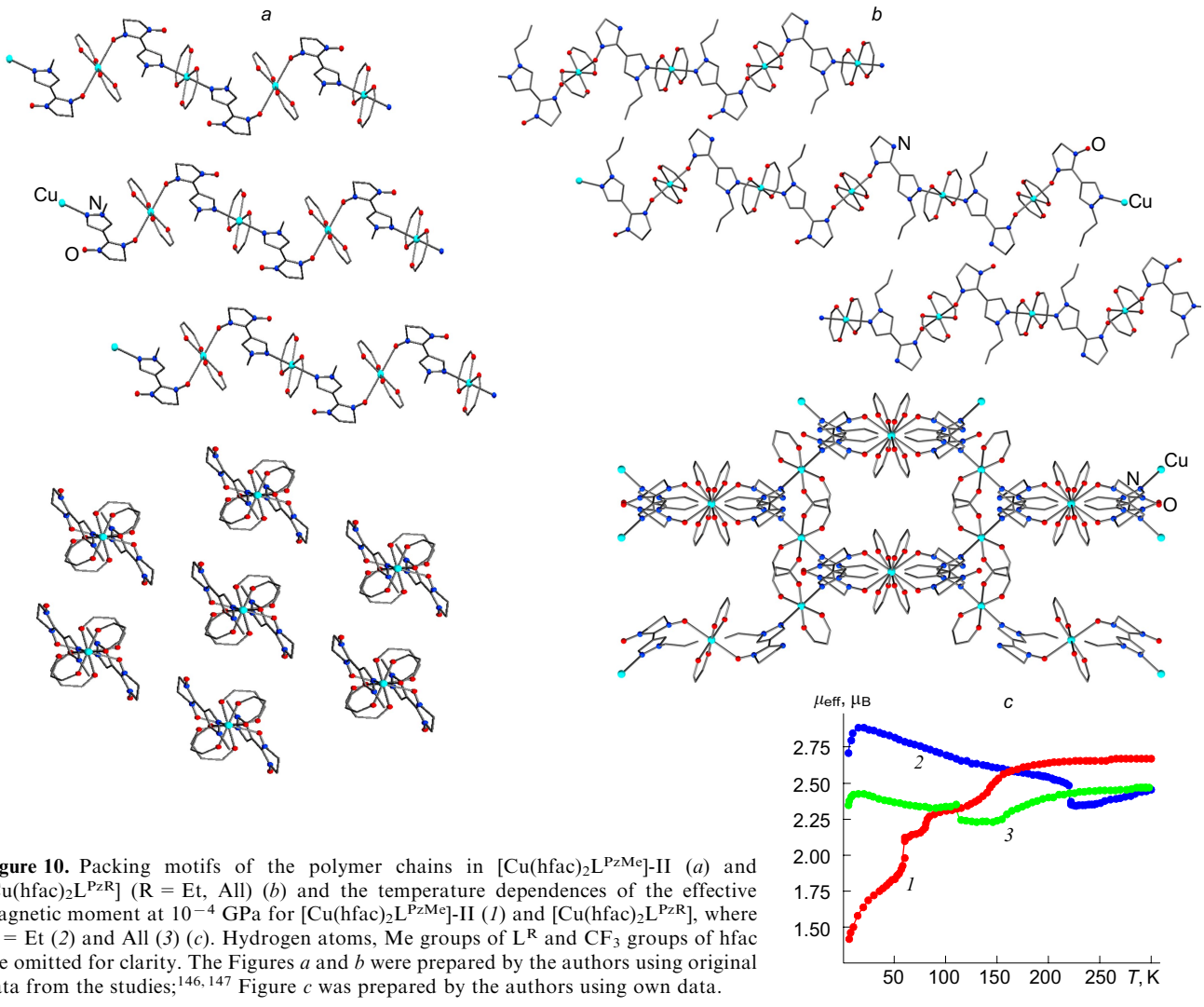



**Figure 10.** Packing motifs of the polymer chains in $[Cu(hfac)_2L^{PzMe}]$-II (*a*) and $[Cu(hfac)_2L^{PzR}]$ (R = Et, All) (*b*) and the temperature dependences of the effective magnetic moment at $10^{-4}$ GPa for $[Cu(hfac)_2L^{PzMe}]$-II (*1*) and $[Cu(hfac)_2L^{PzR}]$, where R = Et (*2*) and All (*3*) (*c*). Hydrogen atoms, Me groups of $L^R$ and $CF_3$ groups of hfac are omitted for clarity. The Figures *a* and *b* were prepared by the authors using original data from the studies;[146, 147] Figure *c* was prepared by the authors using own data.

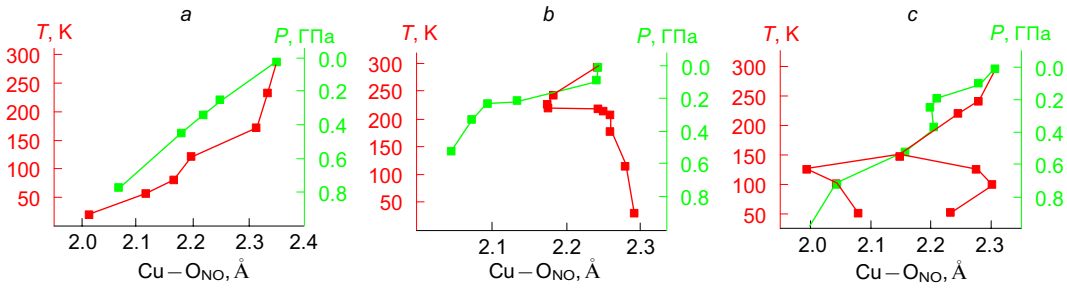



**Figure 11.** Plots of the Cu – $O_{NO}$ distances *versus* the temperature and pressure for $[Cu(hfac)_2L^{PzMe}]$-II (*a*), $[Cu(hfac)_2L^{PzEt}]$ (*b*) and $[Cu(hfac)_2L^{PzAll}]$ (*c*).[146,147] The Figure was prepared by the authors using original data from the studies.[146,147]

Thus, the axial coordination mode of the NO group of the nitroxide changes to an equatorial one. The observed decrease in the Cu – $O_{NO}$ distance on cooling is a consequence of an increase in the fraction of the low-temperature phase, in which the exchange clusters are in the state with a strong antiferromagnetic exchange coupling. Besides, the cooling leads to a significant decrease in the interchain O···O contacts between uncoordinated NO groups of the nitroxide radicals of adjacent chains from 3.902(3) Å at 295 K to 3.572(2) Å at 30 K.

The cooling of the crystals of $[Cu(hfac)_2L^{PzEt}]$ from 300 to 226 K leads to a gradual decrease in the Cu – $O_{NO}$ and Cu – N bond lengths (Fig. 11,*b*), and then at 220 K the Cu – N bond lengths abruptly decrease and the Cu – $O_{NO}$ distances abruptly increase, which account for the non-monotonic change in $\mu_{eff}$. As the temperature is further decreased, the Cu – $O_{NO}$ distances continue to increase and the Cu – N bonds continue to decrease, while the crystal symmetry remains unchanged.[152]

The structural transformation of $[Cu(hfac)_2L^{PzAll}]$ is a more complex process. Thus, the cooling of the sample from 300 to 150 K leads to an insignificant decrease in the Cu – $O_{NO}$ and Cu – N distances (by 0.159 and 0.031 Å, respectively).[151] In the temperature range of 150 – 125 K, the symmetry-lowering structural phase transition occurs giving rise to two types of crystallographically independent chains. In one of these chains, the Cu – $O_{NO}$ distances sharply decrease, while they sharply increase in another chain (see Fig. 11 *c*). This results in that ferromagnetic exchange interactions are dominant in half of exchange clusters, leading to an increase in $\mu_{eff}$ on further cooling. Only the cooling below 122 K leads to the reduction of the Cu – N distances in all $\{CuO_4N_2\}$ coordination units of all chains.[151]

The magnetic behaviour of the samples and crystal structures of these compounds under an applied hydrostatic pressure are also different. The most interesting magnetic structural effect was observed in the crystals of $[Cu(hfac)_2L^{PzMe}]$-II under moderately high pressures (~0.07 GPa). Thus, the application of an external pressure significantly restricted the displacements of atoms in the exchange clusters $\{>N-^{\bullet}O-Cu^{II}-O^{\bullet}-N<\}$, which was manifested in the disappearance of stepwise specific features in the thermomagnetic curve $\mu_{eff}(T,P)$ at 0.07 GPa.[146] The X-ray diffraction study demonstrated that an increase in the external pressure to ~0.04 GPa leads to a decrease in the distance between the $CF_3$ group of one hfac anion and the radical of the same polymer chain. This hinders the migration of the nitroxide radical towards the copper atom, which is necessary for the switching of the state of the exchange cluster, on cooling up to the applied pressure of ~0.14 GPa. A further increase in the pressure to 0.23 GPa and higher leads to the displacement of the $CF_3$ group away from the radical, thereby allowing structural transformations to occur in the exchange cluster. The cooling in the temperature range of 4 – 50 K at a pressure higher than ~0.2 GPa leads to a gradual decrease in $\mu_{eff}$ comparable with that on cooling to < 50 K at $10^{-4}$ GPa.

As mentioned above, the negative linear compressibility is rather rarely observed in magnetically active coordination compounds. Nevertheless, this effect was found in the study of the crystal structure dynamics of $[Cu(hfac)_2L^{PzMe}]$-II. Thus, in the pressure range from $10^{-4}$ to 0.2 GPa, the unit cell parameter *c* was found to increase (Fig. 12 *a*) due to the displacement of adjacent layers of the chains nearly in the [001] direction. This was accompanied by a significant reduction in the O···O contacts between the uncoordinated NO groups of these nitroxide radicals nearly in the [100] direction, which is the direction of the most significant pressure-induced compression. It is worth noting that the reduction in the O···O contact from 3.902(3) to 2.95(1) Å (*i.e.*, by 0.95 Å) (Fig. 12 *b*), induced by the applied pressure of 1.09 GPa, is much larger compared to the decrease of

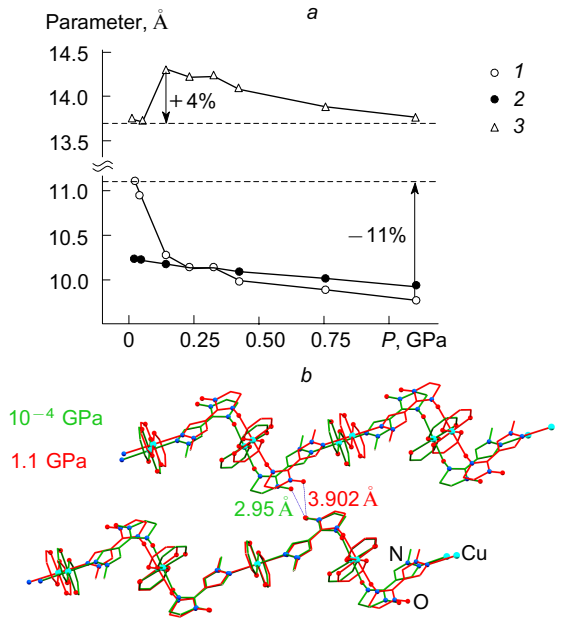



**Figure 12.** Plots of the unit cell parameters *a* (*1*), *b* (*2*) and *c* (*3*) *versus* the pressure (*a*) and the change in the arrangement of nitroxide groups of two adjacent polymer chains with the shortest distances between the chains (*b*) in the structure of $[Cu(hfac)_2L^{PzMe}]$-II (hydrogen atoms and the $CH_3$ and $CF_3$ groups are omitted for clarity). The values +4 and −11% indicate the changes in the parameter with respect to the initial value (at 295 K, 1 atm). The Figure was prepared by the authors using original data from the study.[146]

0.33 Å caused by the cooling at $10^{-4}$ GPa in the temperature range of 300 – 30 K.[146]

The pressure-induced dynamics of the coordination geometry of the copper atom is consistent with the magnetic properties of $[Cu(hfac)_2L^{PzMe}]$-II. The pressure causes a gradual decrease in the $Cu-O_{NO}$ distance (see Fig. 11 *a*), which, like the cooling at $10^{-4}$ GPa, stabilizes the low-spin state of exchange clusters and leads to a decrease in $\mu_{eff}$ at 300 K.

The investigation of the thermomagnetic properties of $[Cu(hfac)_2L^{PzEt}]$ and $[Cu(hfac)_2L^{PzAll}]$ demonstrated[147] that, as in the case of $[Cu(hfac)_2L^{PzMe}]$-II, anomalies of thermomagnetic properties disappear under an applied relatively low hydrostatic pressure of ~0.05 – 0.1 GPa. A higher pressure leads to a change in the character of the $\mu_{eff}(T)$ plot in the temperature range of 50 – 150 K. As in the case of $[Cu(hfac)_2L^{PzMe}]$-II, the external pressure causes a gradual decrease in $\mu_{eff}$ (300 K), resulting in the stabilization of the low-spin state of exchange clusters for all the complexes $[Cu(hfac)_2L^{PzR}]$ under consideration at a pressure of ~1 GPa. The high-pressure X-ray diffraction data for the crystals are in agreement with the thermomagnetic properties of the compounds. Actually, the external pressure causes a monotonic reduction in the $Cu-O_{NO}$ distance.

It should be emphasized that the pressure-induced transformation path of the coordination units of $[Cu(hfac)_2L^{PzEt}]$ (see Fig. 12 *b*) significantly differs from the temperature-induced path. In the structure of $[Cu(hfac)_2L^{PzEt}]$, the Cu – N and $Cu-O_{NO}$ bond lengths are rather rapidly reduced by 0.212 and 0.106 Å, respectively, with increasing pressure to 0.21 GPa and then reach values typical of the equatorially coordinated nitrogen and oxygen atoms [Cu – N = 2.092(8) Å and $Cu-O_{NO}$ = 2.074(6) Å] at 0.32 GPa. An increase in the pressure to 0.52 GPa leads to a further gradual reduction in the Cu – N and $Cu-O_{NO}$ distances by ~0.028 Å. Therefore, the main rearrangement in the metal environment in $[Cu(hfac)_2L^{PzEt}]$ occurs in the pressure range from 0.09 to 0.32 GPa.

In the structure of $[Cu(hfac)_2L^{PzAll}]$, an increase in the pressure to 0.25 GPa leads to a decrease in the Cu – N and $Cu-O_{NO}$ distances by 0.060 and 0.107 Å, respectively. At 0.37 GPa, the Cu – N bond sharply decreases by 0.256 Å, whereas in the temperature range of 0.19 – 0.37 GPa, the $Cu-O_{NO}$ bond length is weakly sensitive to pressure. The further increase in the pressure is accompanied by a gradual reduction in the Cu – N and $Cu-O_{NO}$ distances to 2.043(10) and 1.990(10) Å, respectively, at 1.05 GPa. Hence, an increase in the pressure causes a significant reduction in the Cu – N distances in the crystals of $[Cu(hfac)_2L^{All}]$ and only then a decrease in the $Cu-O_{NO}$ distances.

Therefore, an analysis of the published data shows that the external pressure effects on divalent copper complexes with nitroxide radicals are quite diverse. For some examples, the expected shift of the plot of thermomagnetic properties as a whole to higher temperatures can be observed in accordance with the Clausius – Clapeyron equation.[28] The sensitivity of breathing crystals to external pressure[143, 145] is significantly higher than that of conventional iron compounds exhibiting spin crossover. The suppression of magnetic effects in a number of complexes in the temperature range of 200 – 300 K under an applied relatively low external pressure (up to 0.1 GPa) is indicative of high sensitivity of the magnetic properties of breathing crystals. Therefore, they are promising materials as external pressure sensors. It is worth noting that the stabilization of the high-spin state of compounds exhibiting pressure-induced spin crossover properties is a very rare phenomenon.[46] The ability of breathing crystals to exhibit thermochromic and piezochromic properties deserves attention, especially since both these properties are due to the external stimulus-induced transformation of the coordination environment of the $Cu^{II}$ ion and, correspondingly, of the exchange clusters $\{>N-{}^{\bullet}O-Cu^{II}-O^{\bullet}-N<\}$, resulting in the change of their spin state.[143]

The fact that the pressure of <1 GPa is sufficient to induce the HS ⇄ LS phase transitions in $Cu^{II}$ complexes with nitroxide radicals is attributed to the energetically favourable spin-pairing, which is a remarkable contribution to chemical bonding. Much higher hydrostatic pressures are generally used in studying pressure-induced structural changes in copper complexes with diamagnetic ligands. Since there is abundant literature on copper complexes with diamagnetic ligands,[139, 153 – 170] let us consider only one of such complexes, $[CuF_2(H_2O)_2(pyz)]$,[154] in which the Jahn – Teller axis switching in the coordination environment of the $Cu^{II}$ ion was observed (Fig. 13). This complex is a polymer containing $Cu^{II}$ ions that are bridged by pyrazine (pyz) molecules to form chains. The centrosymmetric environment of copper involves two oxygen atoms, two pyrazine nitrogen atoms and two fluorine anions.

Several pressure-driven transformations occur in the crystals of $[CuF_2(H_2O)_2(pyz)]$.[154] An increase in the pressure to 1.2 GPa causes only slight changes in the Cu – X bond lengths (X = N, F, O). An increase in the pressure to 1.8 GPa leads to the phase transition accompanied by the reorientation of the Jahn – Teller axis, with the symmetry being unchanged. Thus, the Cu – N distances decrease from 2.454(6) to 2.039(3) Å, whereas the $Cu-O_{H_2O}$ bonds are significantly elongated from 1.984(4) to 2.316(3) Å. Upon a further increase in the pressure to 3.3 GPa, the sample undergoes a chemical transformation. Thus, two thirds of the chains lose one water molecule per copper atom and undergo dimerization through fluorine atoms serving as bridges (see Fig. 13 *c*). As a result, two chains are linked together, while the geometry of the third chain remains almost unchanged. This phase transition is reflected in the magnetic properties of the complex.[171] This example clearly demonstrates that a significantly higher external pressure should be applied to change the direction of the Jahn – Teller axis (if this change occurs at all) in divalent copper complexes with diamagnetic ligands compared to that required for complexes with coordinated nitroxide radicals.

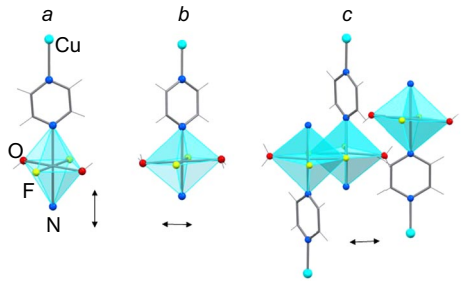



**Figure 13.** Directions of Jahn – Teller axes (indicated by arrows) in Cu octahedra at 300 K and a pressure of $10^{-4}$ (*a*), 2.2 (*b*) and 3.3 GPa (*c*). The Figure was prepared by the authors using original data from the study.[154]

## 7. Conclusion

An interest in new types of functional materials gave impetus to research on the changes in the internal structure of solids induced by an external pressure. The data presented in the review demonstrate that these processes have attracted the growing interest of researchers in different fields. These studies become more common despite the fact that high-pressure experiments (particularly single-crystal X-ray diffraction studies) are associated with challenges and limitations (crystal size limitations, constraints on the data collection area imposed by high-pressure cell geometry, low data completeness, intensity of the X-ray source, *etc.*).[16] To achieve high pressures, researchers use diamond anvil cells of small diameter, which inevitably leads to sample size limitations. The use of high-brilliance and highly collimated synchrotron beams is the only way to obtain high-quality data at ultrahigh pressures. High-pressure experiments at low temperatures also present challenges: accessible regions of reciprocal space, which are limited by the diamond cell, are additionally limited by a cryostat needed for cooling the sample.[26]

Recent progress in this field is largely due to the development of beamlines for high-pressure research at synchrotron radiation facilities.[172]

Besides, multispin compounds, the intracrystalline dynamics in which can be induced without using extremely high pressure, have attracted increasing attention. In many cases, the application of hydrostatic pressure of 0.5 – 1 GPa is quite sufficient for the phase transition to occur. These transitions are reversible and do not lead to the chemical decomposition of the compound. Hence, the conversion of the spin state potentially can be responsible for the functional activity of the compound serving as the data storage media, external stimulus-responsive sensors or actuators for certain solid-state processes. In addition, multispin structures show unusual structural dynamics, which is not inherent in the nature of diamagnetic compounds. This issue is of independent interest. Pressure-induced structural changes in these compounds can follow the pathway, which is different from that of temperature-induced transformations and is accompanied by a qualitative difference in the pressure-induced thermomagnetic properties. Therefore, high-pressure structural data are of great importance. The pressure-induced manifestation of new physical effects, which are inaccessible at atmospheric pressure, have a value in and of themselves.[11, 39, 81, 90, 136, 147, 172]

In this review, we sought to highlight the effect of the pressure applied to crystals of magnetically active compounds on their structures and magnetic properties, without consideration of technical details of experiments and the comparison of such fine structural transformation as changes in anisotropic displacement ellipsoids, which are not always reported in original publications. Details of structural experiments (types of cells, radiation sources, temperature regimes, *etc.*) are available in the cited studies. More systematic data on the technical details of high-pressure experiments are given in recent publications (see, for example, the studies [1, 4, 5, 15 – 18, 22, 24, 168]).

A limited number of available examples and disparate data do not allow one to draw general conclusions. Probably, the rapidly growing number of such studies [173 – 179] will make it possible to reveal common features of magnetic structural effects and predict their occurrence.

This review was written with the financial support of the Russian Science Foundation (Project No. 17-13-01022) and the partial financial support of the Russian Foundation for Basic Research (Project No. 19-29-08005).

## 8. List of abbreviations and acronyms

3,5-Cat — 3,5-di(*tert*-butyl)-*o*-benzoquinone dianion,
3,5-SQ — 3,5-di(*tert*-butyl)-*o*-benzoquinone radical anion,
3,6-DBSQ-4,5-$(MeO)_2$ — 3,6-di(*tert*-butyl)-4,5-dimethoxy-1,2-benzoquinone radical anion,
3-CNpy — 3-cyanopyridine,
abpt — 4-amino-3,5-bis(pyridin-2-yl)-1,2,4-triazole,
bipy — 2,2′-bipyridyl,
btr — 4,4′-bis(1,2,4-triazole),
btz — 2,2′-bis(4,5-dihydrothiazine),
CC — coordination compound,
CSD — Cambridge Structural Database,
dhbq — deprotonated 2,5-dihydroxy-*p*-benzoquinone,
diox — 9,10-dioxophenanthrene,
dpp — dipyrido[3,2-*a*:2′3′-c]phenazine,
dpqa — bis(2-pyridylmethyl)-*N*-(quinolin-2-ylmethyl)-amine,
EXAFS — extended X-ray absorption fine structure,
$H_3$cht — *cis*,*cis*-cyclohexane-1,3,5-triol,
hfac — hexafluoroacetylacetonate,
HS — high-spin state,
LCC — linear compressibility coefficient,
LIESST — light-induced excited spin-state trapping,
LS — low-spin state,
$LS_P$ — high-pressure low-spin phase,
$LS_T$ — low-temperature low-spin phase,
$O_2$C-naphth — naphtholate anion,
phen — phenanthroline,
pmd — pyrimidine,
pyz — pyrazine,
Pz — pyrazole,
$Rsao^{2-}$ — R-substituted salicylaldoxime dianion,
Solv — solvent molecule in the crystal solvate,
TEC— thermal expansion coefficient,
THF — tetrahydrofuran,
XANES — X-ray absorption near edge structure,
XRD — X-ray diffraction,
$D$ — parameter characterizing magnetic anisotropy,
$\Delta H_{HL}$ — change in the enthalpy difference between high- and low-spin phases,
$\Delta S_{HL}$ — change in the molar entropy upon a phase transition,
$\Delta V_{HL}$ — difference between the molar volumes of the high- and low-spin phases near the equilibrium position,
$l$ — size of the body in a certain direction,
$P$ — external pressure,
$T_c$ — transition temperature,
$T_{1/2}$ — temperature, at which half of the total amount of spin-changing molecules are in the LS state,
$\mu_{ef}$ — effective magnetic moment,
$\chi$ — magnetic susceptibility.

## 9. References

1. J.S.Tse. *Natl. Sci. Rev.*, **7**, 149 (2020)
2. J.R.Helliwell. *Acta Crystallogr., Sect. D: Struct. Biol.*, **76**, 87 (2020)
3. C.E.Kundrot, F.M.Richards. *J. Mol. Biol.*, **193**, 157 (1987)
4. K.Kurpiewska, K.Lewiński. *Open Life Sci.*, **5**, 531 (2010)
5. N.Watanabe. In *High Pressure Bioscience. Subcellular Biochemistry*. (Eds K.Akasaka, H.Matsuki). (Dordrecht: Springer-Verlag, 2015). P. 677

6. F.Colmenero. *Mater. Adv.*, **1**, 1399 (2020)
7. X.Huang, X.Wang, D.Duan, B.Sundqvist, X.Li, Y.Huang, H.Yu, F.Li, Q.Zhou, B.Liu, T.Cui. *Natl. Sci. Rev.*, **6**, 713 (2019)
8. E.Snider, N.Dasenbrock-Gammon, R.McBride, M.Debessai, H.Vindana, K.Vencatasamy, K.V.Lawler, A.Salamat, R.P.Dias. *Nature (London)*, **586**, 373 (2020)
9. L.Seixas, A.S.Rodin, A.Carvalho, A.H.Castro Neto. *Phys. Rev. B*, **91**, 115437 (2015)
10. Y.Ma, M.Eremets, A.R.Oganov, Y.Xie, I.Trojan, S.Medvedev, A.O.Lyakhov, M.Valle, V.Prakapenka. *Nature (London)*, **458**, 182 (2009)
11. V.Ovcharenko, E.Bagryanskaya. In *Spin-Crossover Materials*. (Ed. M.A.Halcrow). (Oxford: Wiley, 2013). P. 239
12. *Molecular Magnetic Materials*. (Eds B.Sieklucka, D.Pinkowicz). (Weinheim: Wiley-VCH, 2017)
13. A.I.Aleksandrov, I.A.Alexandrov, A.I.Prokof'ev. *JETP Lett.*, **97**, 546 (2013)
14. A.I.Aleksandrov, V.G.Shevchenko, I.A.Aleksandrov, S.V.Fokin, V.I.Ovcharenko. *Techn. Phys. Lett.*, **47**, 19 (2021)
15. E.V.Boldyreva. In *High-Pressure Crystallography: From Fundamental Phenomena to Technological Applications*. (Eds E.Boldyreva, P.Dera). (Dordrecht: Springer, 2010). P. 612
16. P.F.McMillan. In *High-Pressure Crystallography*. (Eds A.Katrusiak, P.McMillan). (Dordrecht: Springer, 2004). P. 367
17. B.A.Zakharov, E.V.Boldyreva. *CrystEngComm*, **21**, 10 (2019)
18. A.M.Thiel, E.Damgaard-Møller, J.Overgaard. *Inorg. Chem.*, **59**, 1682 (2020)
19. J.P.Tidey, H.L.S.Wong, M.Schröder, A.J.Blake. *Coord. Chem. Rev.*, **277**, 187 (2014)
20. V.I.Ovcharenko, G.V.Romanenko, K.Y.Maryunina, A.S.Bogomyakov, E.V.Gorelik. *Inorg. Chem.*, **47**, 9537 (2008)
21. V.Ovcharenko. In *Stable Radicals*. (Ed. R.Hicks). (Chichester: Wiley, 2010). P. 461
22. J.Sanchez-Benitez, S.Tancharakorn, M.K.Hutchison, K.V.Kamenev. *J. Phys. Conf. Ser.*, **121**, 122001 (2008)
23. M.Lesik, T.Plisson, L.Toraille, J.Renaud, F.Occelli, M.Schmidt, O.Salord, A.Delobbe, T.Debuisschert, L.Rondin, P.Loubeyre, J.-F.Roch. *Science*, **366**, 1359 (2019)
24. I.N.Goncharenko. In *High-Pressure Crystallography*. (Eds A.Katrusiak, P.McMillan). (Dordrecht: Springer, 2004). P. 321
25. M.D.Manrique-Juárez, S.Rat, L.Salmon, G.Molnár, C.M.Quintero, L.Nicu, H.J.Shepherd, A.Bousseksou. *Coord. Chem. Rev.*, **308**, 395 (2016)
26. C.J.Ridley, K.V.Kamenev. *Z. Kristallogr.*, **229**, 171 (2014)
27. J.A.Rodríguez-Velamazán, L.Cañadillas-Delgado, M.Castro, G.J.McIntyre, J.A.Real. *Acta Crystallogr., Sect. B: Struct. Sci. Cryst. Eng. Mater.*, **70**, 436 (2014)
28. A.B.Gaspar, G.Molnár, A.Rotaru, H.J.Shepherd. *C. R. Acad. Sci., Ser. IIC: Chim.*, **21**, 1095 (2018)
29. C.R.Groom, I.J.Bruno, M.P.Lightfoot, S.C.Ward. *Acta Crystallogr., Sect. B: Struct. Sci. Cryst. Eng. Mater.*, **72**, 171 (2016)
30. L.Cambi, L.Szegö. *Ber. Dtsch. Chem. Ges.*, **64**, 2591 (1931)
31. A.Hauser. In *Spin Crossover in Transition Metal Compounds. I. Topics in Current Chemistry*. Vol. 233. (Berlin, Heidelberg: Springer, 2012). P. 49
32. H.Spiering, K.Boukheddaden, J.Linares, F.Varret. *Phys. Rev. B*, **70**, 184106 (2004)
33. P.Gütlich, A.Hauser, H.Spiering. *Angew. Chem., Int. Ed. Engl.*, **33**, 2024 (1994)
34. P.Mounaix, E.Freysz, J.Degert, N.Daro, J.-F.Létard, P.Kužel, V.Vigneras, L.Oyenhart. *Appl. Phys. Lett.*, **89**, 174105 (2006)
35. S.Bonhommeau, T.Guillon, L.M.Lawson Daku, P.Demont, J.Sanchez Costa, J.-F.Létard, G.Molnár, A.Bousseksou. *Angew. Chem., Int. Ed.*, **45**, 1625 (2006)
36. A.Bousseksou, G.Molnár, P.Demont, J.Menegotto. *J. Mater. Chem.*, **13**, 2069 (2003)
37. A.Hauser. *Chem. Phys. Lett.*, **202**, 173 (1993)
38. E.D.Loutete-Dangui, F.Varret, E.Codjovi, P.R.Dahoo, H.Tokoro, S.Ohkoshi, C.Eypert, J.F.Létard, J.M.Coanga, K.Boukheddaden. *Phys. Rev. B*, **75**, 184425 (2007)
39. M.A.Halcrow. *Chem. Soc. Rev.*, **40**, 4119 (2011)
40. M.A.Halcrow, I.Capel Berdiell, C.M.Pask, R.Kulmaczewski. *Inorg. Chem.*, **58**, 9811 (2019)
41. G.Levchenko, G.Bukin, H.Fylymonov, Q.Li, A.B. Gaspar, J.A.Real. *J. Phys. Chem. C*, **123**, 5642 (2019)
42. P.Guionneau, C.Brigouleix, Y.Barrans, A.E.Goeta, J.-F.Létard, J.A.K.Howard, J.Gaultier, D.Chasseau. *C. R. Acad. Sci., Ser. IIC: Chem.*, **4**, 161 (2001)
43. H.Shepherd, G.Tonge, L.Hatcher, M.Bryant, J.Knichal, P.Raithby, M.Halcrow, R.Kulmaczewski, K.Gagnon, S.Teat. *Magnetochemistry*, **2**, 9 (2016)
44. T.Granier, B.Gallois, J.Gaultier, J.A.Real, J.Zarembowitch. *Inorg. Chem.*, **32**, 5305 (1993)
45. H.E.Mason, W.Li, M.A.Carpenter, M.L.Hamilton, J.A.K.Howard, H.A.Sparkes. *New J. Chem.*, **40**, 2466 (2016)
46. P.Gutlih, V.Ksenofontov, A.Gaspar. *Coord. Chem. Rev.*, **249**, 1811 (2005)
47. J.A.Rodríguez-Velamazán, O.Fabelo, C.M.Beavers, E.Natividad, M.Evangelisti, O.Roubeau. *Chem. – Eur. J.*, **20**, 7956 (2014)
48. H.J.Shepherd, T.Palamarciuc, P.Rosa, P.Guionneau, G.Molnár, J.F.Létard, A.Bousseksou. *Angew. Chem., Int. Ed.*, **51**, 3910 (2012)
49. D.Pinkowicz, M.Rams, M.Mišek, K.V.Kamenev, H.Tomkowiak, A.Katrusiak, B.Sieklucka. *J. Am. Chem. Soc.*, **137**, 8795 (2015)
50. G.G.Levchenko, A. V.Khristov, V.N.Varyukhin. *Low Temp. Phys.*, **40**, 571 (2014)
51. P.Guionneau, M.Marchivie, G.Bravic, J.-F.Létard, D.Chasseau. In *Spin Crossover Transition in Metal Compounds. II. Topics in Current Chemistry*. Vol. 234. (Eds P.Gütlich, H.A.Goodwin). (Springer-Verlag, 2004). P. 97
52. G.Molnár, S.Rat, L.Salmon, W.Nicolazzi, A.Bousseksou. *Adv. Mater.*, **30**, 1 (2018)
53. C.P.Köhler, R.Jakobi, E.Meissner, L.Wiehl, H.Spiering, P.Gütlich. *J. Phys. Chem. Solids*, **51**, 239 (1990)
54. V.Ksenofontov, G.Levchenko, H.Spiering, P.Gütlich, J.-F.Létard, Y.Bouhedja, O.Kahn. *Chem. Phys. Lett.*, **294**, 545 (1998)
55. A.B.Gaspar, M.C.Muñoz, N.Moliner, V.Ksenofontov, G.Levchenko, P.Gütlich, J.A.Real. *Monatsh. Chem.*, **134**, 285 (2003)
56. V.Ksenofontov, A.B.Gaspar, G.Levchenko, B.Fitzsimmons, P.Gütlich. *J. Phys. Chem. B*, **108**, 7723 (2004)
57. A.B.Gaspar, G.Agustí, V.Martínez, M.C.Muñoz, G.Levchenko, J.A.Real. *Inorg. Chim. Acta*, **358**, 4089 (2005)
58. A.Galet, A.B.Gaspar, G.Agusti, M.C.Muñoz, G.Levchenko, J.A.Real. *Eur. J. Inorg. Chem.*, 3571 (2006)
59. B.Li, R.-J.Wei, J.Tao, R.-B.Huang, L.-S.Zheng. *Inorg. Chem.*, **49**, 745 (2010)
60. A.Sugahara, K.Moriya, M.Enomoto, A.Okazawa, N.Kojima. *Polyhedron*, **30**, 3127 (2011)
61. F.-L.Yang, B.Li, T.Hanajima, Y.Einaga, R.-B.Huang, L.-S.Zheng, J.Tao. *Dalton Trans.*, **39**, 2288 (2010)
62. N.F.Sciortino, S.M.Neville, C.Desplanches, J.-F.Létard, V.Martinez, J.A.Real, B.Moubaraki, K.S.Murray, C.J.Kepert. *Chem. – Eur. J.*, **20**, 7448 (2014)
63. A.Bouseksou, G.Molnár, G.Matouzenko. *Eur. J. Inorg. Chem.*, 4353 (2004)
64. K.Babilotte, K.Boukheddaden. *Phys. Rev. B*, **101**, 174113 (2020)
65. M.Marchivie, P.Guionneau, J.A.K.Howard, G.Chastanet, J.-F.Létard, A.E.Goeta, D.Chasseau. *J. Am. Chem. Soc.*, **124**, 194 (2002)

66. B.Gallois, C.Hauw, J.A.Real, J.Zarembowitch. *Inorg. Chem.*, **29**, 1152 (1990)
67. P.Spacu, D.Ciomartan, M.Teodorescu. *Rev. Roum. Chim.*, **17**, 977 (1972)
68. V.Legrand, S.Pillet, H.-P.Weber, M.Souhassou, J.-F.Létard, P.Guionneau, C.Lecomte. *J. Appl. Crystallogr.*, **40**, 1076 (2007)
69. S.Pillet, V.Legrand, H.-P.Weber, M.Souhassou, J.-F.Létard, P.Guionneau, C.Lecomte. *Z. Kristallogr.*, **223**, 235 (2008)
70. J.-J.Lee, H.Sheu, C.-R.Lee, J.-M.Chen, J.-F.Lee, C.-C.Wang, C.-H.Huang, Y.Wang. *J. Am. Chem. Soc.*, **122**, 5742 (2000)
71. E.König, K.Madeja. *J. Chem. Soc. Chem. Commun. (London)*, 61 (1966)
72. J.A.Real, A.B.Gaspar, V.Niel, M.C.Muñoz. *Coord. Chem. Rev.*, **236**, 121 (2003)
73. M.Konno, M.Mikami-Kido. *Bull. Chem. Soc. Jpn.*, **64**, 339 (1991)
74. A.L.Goodwin, D.A.Keen, M.G.Tucker. *Proc. Natl. Acad. Sci., USA*, **105**, 18708 (2008)
75. A.B.Cairns, A.L.Thompson, M.G.Tucker, J.Haines, A.L.Goodwin. *J. Am. Chem. Soc.*, **134**, 4454 (2012)
76. A.D.Fortes, E.Suard, K.S.Knight. *Science*, **331**, 742 (2011)
77. J.Kusz, M.Zubko, A.Fitch, P.Gütlich. *Z. Kristallogr.*, **226**, 576 (2011)
78. Y.Garcia, V.Ksenofontov, G.Levchenko, G.Schmitt, P.Gütlich. *J. Phys. Chem. B*, **104**, 5045 (2000)
79. S.Chorazy, T.Charytanowicz, D.Pinkowicz, J.Wang, K.Nakabayashi, S.Klimke, F.Renz, S.Ohkoshi, B.Sieklucka. *Angew. Chem., Int. Ed.*, **59**, 15741 (2020)
80. G.Handzlik, B.Sieklucka, H.Tomkowiak, A.Katrusiak, D.Pinkowicz. *Magnetochemistry*, **5**, 33 (2019)
81. S.Chorazy, J.J.Zakrzewski, M.Magott, T.Korzeniak, B.Nowicka, D.Pinkowicz, R.Podgajny, B.Sieklucka. *Chem. Soc. Rev.*, **49**, 5945 (2020)
82. O.Sato, T.Iyoda, A.Fujishima, K.Hashimoto. *Science*, **272**, 704 (1996)
83. S.Ohkoshi, K.Imoto, Y.Tsunobuchi, S.Takano, H.Tokoro. *Nat. Chem.*, **3**, 564 (2011)
84. P.Gütlich. *Eur. J. Inorg. Chem.*, 581 (2013)
85. H.Y.Sun, Y.S.Meng, T.Liu. *Chem. Commun.*, **55**, 8359 (2019)
86. T.Liu, Y.-J.Zhang, S.Kanegawa, O.Sato. *J. Am. Chem. Soc.*, **132**, 8250 (2010)
87. N.Hoshino, F.Iijima, G.N.Newton, N.Yoshida, T.Shiga, H.Nojiri, A.Nakao, R.Kumai, Y.Murakami, H.Oshio. *Nat. Chem.*, **4**, 921 (2012)
88. O.Sato. *Proc. Jpn. Acad., Ser. B*, **88**, 213 (2012)
89. S.Decurtins, P.Gütlich, C.P.Köhler, H.Spiering, A.Hauser. *Chem. Phys. Lett.*, **105**, 1 (1984)
90. D.Pinkowicz, R.Pełka, O.Drath, W.Nitek, M.Bałanda, A.M.Majcher, G.Poneti, B.Sieklucka. *Inorg. Chem.*, **49**, 7565 (2010)
91. B.Li, F.L.Yang, J.Tao, O.Sato, R.Bin Huang, L.S.Zheng. *Chem. Commun.*, 6019 (2008)
92. V.Ksenofontov, A.B.Gaspar, P.Gütlich. In *Spin Crossover Transition in Metal Compounds. III. Topics in Current Chemistry*. Vol. 235. (Berlin, Heidelberg: Springer-Verlag, 2003). P. 23
93. C.Roux, D.M.Adams, J.P.Itié, A.Polian, D.N.Hendrickson, M.Verdaguer. *Inorg. Chem.*, **35**, 2846 (1996)
94. A.Caneschi, A.Dei, F.Fabrizi De Biani, P.Gütlich, V.Ksenofontov, G.Levchenko, A.Hoefer, F.Renz. *Chem. – Eur. J.*, **7**, 3926 (2001)
95. E.Evangelio, D.Ruiz-Molina. *Eur. J. Inorg. Chem.*, 2957 (2005)
96. O.-S.Jung, C.G.Pierpont. *Inorg. Chem.*, **33**, 2227 (1994)
97. J.Overgaard, L.H.Møller, M.A.Borup, M.Tricoire, J.P.S.Walsh, M.Diehl, E.Rentschler. *Dalton Trans.*, **45**, 12924 (2016)
98. V.V.Novikov, Y.V.Nelyubina. *Russ. Chem. Rev.*, **90**, 1330 (2021)
99. V.I.Ovcharenko, O.V.Kuznetsova. *Russ. Chem. Rev.*, **89**, 1261 (2020)
100. C.J.Milios, R.Inglis, A.Vinslava, R.Bagai, W.Wernsdorfer, S.Parsons, S.P.Perlepes, G.Christou, E.K.Brechin. *J. Am. Chem. Soc.*, **129**, 12505 (2007)
101. A.Prescimone, C.J.Milios, J.Sanchez-Benitez, K.V.Kamenev, C.Loose, J.Kortus, S.Moggach, M.Murrie, J.E.Warren, A.R.Lennie, S.Parsons, E.K.Brechin. *Dalton Trans.*, 4858 (2009)
102. 1A.Prescimone, J.Sanchez-Benitez, K.V.Kamenev, S.A.Moggach, A.R.Lennie, J.E.Warren, M.Murrie, S.Parsons, E.K.Brechin. *Dalton Trans.*, 7390 (2009)
103. Y.Sato, H.Miyasaka, N.Matsumoto, H.Ōkawa. *Inorg. Chim. Acta*, **247**, 57 (1996)
104. H.Miyasaka, R.Clérac, T.Ishii, H.-C.Chang, S.Kitagawa, M.Yamashita. *Dalton Trans.*, 1528 (2002)
105. H.Miyasaka, K.Mizushima, S.Furukawa, K.-I.Sugiura, T.Ishii, M.Yamashita. *Mol. Cryst. Liq. Cryst.*, **379**, 171 (2002)
106. J.Yamauchi, K.Takeda, K.Konishi. *Mol. Cryst. Liq. Cryst. Sci. Technol., Sect. A: Mol. Cryst. Liq. Cryst.*, **233**, 97 (1993)
107. M.Mito, M.Hitaka, T.Kawae, K.Takeda, K.Suzuki, K.Mukai. *Mol. Cryst. Liq. Cryst. Sci. Technol., Sect. A: Mol. Cryst. Liq. Cryst.*, **334**, 369 (1999)
108. K.Awaga, Y.Maruyama. *Chem. Mater.*, **2**, 535 (1990)
109. D.Tian, S.M.Winter, A.Mailman, J.W.L.Wong, W.Yong, H.Yamaguchi, Y.Jia, J.S.Tse, S.Desgreniers, R.A.Secco, S.R.Julian, C.Jin, M.Mito, Y.Ohishi, R.T.Oakley. *J. Am. Chem. Soc.*, **137**, 14136 (2015)
110. R.I.Thomson, C.M.Pask, G.O.Lloyd, M.Mito, J.M.Rawson. *Chem. – Eur. J.*, **18**, 8629 (2012)
111. Y.Hosokoshi, M.Tamura, M.Kinoshita. *Mol. Cryst. Liq. Cryst. Sci. Technol., Sect. A: Mol. Cryst. Liq. Cryst.*, **306**, 423 (1997)
112. M.Kinoshita. *Philos. Trans. R. Soc. London., Ser. A: Math. Phys. Eng. Sci.*, **357**, 2855 (1999)
113. Y.Hosokoshi, K.Inoue. *Synth. Met.*, **103**, 2323 (1999)
114. M.Mito, T.Kawae, M.Takumi, K.Nagata, M.Tamura, M.Kinoshita, K.Takeda. *Phys. Rev. B*, **56**, R14255 (1997)
115. K.Takeda, K.Konishi, M.Tamura, M.Kinoshita. *Phys. Rev. B*, **53**, 3374 (1996)
116. K.Takeda, M.Mito, T.Kawae, M.Takumi, K.Nagata, M.Tamura, M.Kinoshita. *J. Phys. Chem. B*, **102**, 671 (1998)
117. M.Mito, T.Kawae, M.Hitaka, K.Takeda, T.Ishida, T.Nogami. *Chem. Phys. Lett.*, **333**, 69 (2001)
118. M.Mito, H.Deguchi, T.Tanimoto, T.Kawae, S.Nakatsuji, H.Morimoto, H.Anzai, H.Nakao, Y.Murakami, K.Takeda. *Phys. Rev. B*, **67**, 2 (2003)
119. N.E.Bogdanov, V.Milašinović, B.A.Zakharov, E.V.Boldyreva, K.Molčanov. *Acta Crystallogr., Sect. B: Struct. Sci. Cryst. Eng. Mater.*, **76**, 285 (2020)
120. K.Lekin, S.M.Winter, L.E.Downie, X.Bao, J.S.Tse, S.Desgreniers, R.A.Secco, P.A.Dube, R.T.Oakley. *J. Am. Chem. Soc.*, **132**, 16212 (2010)
121. K.Lekin, H.Phan, S.M.Winter, J.W.L.Wong, A.A.Leitch, D.Laniel, W.Yong, R.A.Secco, J.S.Tse, S.Desgreniers, P.A.Dube, M.Shatruk, R.T.Oakley. *J. Am. Chem. Soc.*, **136**, 8050 (2014)
122. K.Molčanov, B.Kojić-Prodić. *CrystEngComm*, **19**, 1801 (2017)
123. P.Naumov, J.P.Hill, K.Sakurai, M.Tanaka, K.Ariga. *J. Phys. Chem. A*, **111**, 6449 (2007)
124. K.Molčanov, B.Kojić-Prodić, D.Babić, D.Žilić, B.Rakvin. *CrystEngComm*, **13**, 5170 (2011)
125. E.V.Tretyakov,V.I.Ovcharenko. *Russ. Chem. Rev.*, **78**, 1051 (2009)
126. Y.Hosokoshi, M.Mito, M.Tamura, K.Takeda, K.Inoue, M.Kinoshitat. *Rev. High Press. Sci. Technol.*, **7**, 620 (1998)
127. A.Mailman, S.M.Winter, X.Yu, C.M.Robertson, W.Yong, J.S.Tse, R.A.Secco, Z.Liu, P.A.Dube, J.A.K.Howard, R.T.Oakley. *J. Am. Chem. Soc.*, **134**, 9886 (2012)
128. H.Phan, K.Lekin, S.M.Winter, R.T.Oakley, M.Shatruk. *J. Am. Chem. Soc.*, **135**, 15674 (2013)
129. M.Kertesz. *Chem. – Eur. J.*, **25**, 400 (2019)

130. K.Molčanov, C.Jelsch, B.Landeros, J.Hernández-Trujillo, E.Wenger, V.Stilinović, B.Kojić-Prodić, E.C.Escudero-Adán. *Cryst. Growth Des.*, **19**, 391 (2019)
131. M.Mitsumi, Y.Miyasaki, Y.Kitagawa. *Nihon Kessho Gakkaishi*, **58**, 145 (2016)
132. M.Mitsumi, T.Nishitani, S.Yamasaki, N.Shimada, Y.Komatsu, K.Toriumi, Y.Kitagawa, M.Okumura, Y.Miyazaki, N.Górska, A.Inaba, A.Kanda, N.Hanasaki. *J. Am. Chem. Soc.*, **136**, 7026 (2014)
133. K.Suzuki, Y.Hosokoshi, K.Inoue. *Chem. Lett.*, **31**, 316 (2002)
134. K.Suzuki, Y.Hosokoshi, K.Inoue. *Mol. Cryst. Liq. Cryst.*, **334**, 511 (1999)
135. K.Inoue, F.Iwahori, A.S.Markosyan, H.Iwamura. *Coord. Chem. Rev.*, **198**, 219 (2000)
136. Y.Hosokoshi, K.Suzuki, F.Iwahori, K.Inoue. In *Annual Review 2001*. (Okazaki: National Institute of Nature Sciences; Institute for Molecular Science, 2001). P. 113
137. V.Laukhin, B.Martínez, J.Fontcuberta, D.B.Amabilino, M.Minguet, J.Veciana. *J. Phys. Chem. B*, **108**, 18441 (2004)
138. K.Suzuki, Y.Hosokoshi, K.Inoue. *Mol. Cryst. Liq. Cryst. Sci. Technol., Sect. A: Mol. Cryst. Liq. Cryst.*, **379**, 247 (2002)
139. M.A.Halcrow. *Chem. Soc. Rev.*, **42**, 1784 (2013)
140. R.N.Musin, P.V.Schastnev, S.A.Malinovskaya. *Inorg. Chem.*, **31**, 4118 (1992)
141. W.Kaszub, A.Marino, M.Lorenc, E.Collet, E.G.Bagryanskaya, E.V.Tretyakov, V.I.Ovcharenko, M.V.Fedin. *Angew. Chem., Int. Ed.*, **53**, 10636 (2014)
142. S.E.Tolstikov, N.A.Artiukhova, G.V.Romanenko, A.S.Bogomyakov, E.M.Zueva, I.Y.Barskaya, M.V.Fedin, K.Y.Maryunina, E.V.Tretyakov, R.Z.Sagdeev, V.I.Ovcharenko. *Polyhedron*, **100**, 132 (2015)
143. N.A.Artiukhova, G.V.Romanenko, A.S.Bogomyakov, I.Y.Barskaya, S.L.Veber, M.V.Fedin, K.Y.Maryunina, K.Inoue, V.I.Ovcharenko. *J. Mater. Chem. C*, **4**, 11157 (2016)
144. I.Y.Drozdyuk, K.Y.Maryunina, R.Z.Sagdeev, V.I.Ovcharenko, E.G.Bagryanskaya, M.V.Fedin. *Mol. Phys.*, **111**, 2903 (2013)
145. K.Y.Maryunina, X.Zhang, S.Nishihara, K.Inoue, V.A.Morozov, G.V.Romanenko, V.I.Ovcharenko. *J. Mater. Chem. C*, **3**, 7788 (2015)
146. V.Ovcharenko, G.Romanenko, A.Polushkin, G.Letyagin, A.Bogomyakov, M.Fedin, K.Maryunina, S.Nishihara, K.Inoue, M.Petrova, V.Morozov, E.Zueva. *Inorg. Chem.*, **58**, 9187 (2019)
147. G.V.Romanenko, G.A.Letyagin, K.Y.Maryunina, A.S.Bogomyakov, S.Nishihara, K.Inoue, V.I.Ovcharenko. *Russ. Chem. Bull.*, **69**, 1530 (2020)
148. V.I.Ovcharenko, K.Y.Maryunina, S.V.Fokin, E.V.Tretyakov, G.V.Romanenko, V.N.Ikorskii. *Russ. Chem. Bull.*, **53**, 2406 (2004)
149. S.Fokin, V.Ovcharenko, G.Romanenko, V.Ikorskii. *Inorg. Chem.*, **43**, 969 (2004)
150. I.Fomina, Z.Dobrokhotova, G.Aleksandrov, A.Bogomyakov, M.Fedin, A.Dolganov, T.Magdesieva, V.Novotortsev, I.Eremenko. *Polyhedron*, **29**, 1734 (2010)
151. K.Y.Maryunina, G.V.Romanenko, E.M.Zueva, S.V.Fokin, A.S.Bogomyakov, V.I.Ovcharenko. *Russ. Chem. Bull.*, **62**, 2337 (2013)
152. V.I.Ovcharenko, S.V.Fokin, G.V.Romanenko, V.N.Ikorskii, E.V.Tretyakov, S.F.Vasilevsky, R.Z.Sagdeev. *Mol. Phys.*, **100**, 1107 (2002)
153. K.W.Galloway, S.A.Moggach, P.Parois, A.R.Lennie, J.E.Warren, E.K.Brechin, R.D.Peacock, R.Valiente, J.González, F.Rodríguez, S.Parsons, M.Murrie. *CrystEngComm*, **12**, 2516 (2010)
154. A.Prescimone, C.Morien, D.Allan, J.A.Schlueter, S.W.Tozer, J.L.Manson, S.Parsons, E.K.Brechin, S.Hill. *Angew. Chem., Int. Ed.*, **51**, 7490 (2012)
155. A.Aguirrechu-Comerón, P.Rodríguez-Hernández, U.R.Rodríguez-Mendoza, O.Vallcorba, A.Muñoz, S.Perruchas, J.Gonzalez-Platas. *High Press. Res.*, **39**, 69 (2019)
156. A.Prescimone, J.Sanchez-Benitez, K.K.Kamenev, S.A.Moggach, J.E.Warren, A.R.Lennie, M.Murrie, S.Parsons, E.K.Brechin. *Dalton Trans.*, **39**, 113 (2010)
157. C.J.McMonagle, P.Comar, G.S.Nichol, D.R.Allan, J.González, J.A.Barreda Argüeso, F.Rodríguez, R.Valiente, G.F.Turner, E.K.Brechin, S.A.Moggach. *Chem. Sci.*, **11**, 8793 (2020)
158. J.A.Gould, M.J.Rosseinsky, S.A.Moggach. *Dalton Trans.*, **41**, 5464 (2012)
159. A.J.Graham, J.-C.Tan, D.R.Allan, S.A.Moggach. *Chem. Commun.*, **48**, 1535 (2012)
160. S.C.McKellar, A.J.Graham, D.R.Allan, M.I.H.Mohideen, R.E.Morris, S.A.Moggach. *Nanoscale*, **6**, 4163 (2014)
161. N.Giordano, C.M.Beavers, K.V.Kamenev, J.B.Love, J.R.Pankhurst, S.J.Teat, S.Parsons. *Chem. Commun.*, **56**, 3449 (2020)
162. I.E.Collings, M.Bykov, E.Bykova, M.Hanfland, S.Van Smaalen, L.Dubrovinsky, N.Dubrovinskaia. *CrystEngComm*, **20**, 3512 (2018)
163. A.Aguirrechu-Comerón, R.Hernández-Molina, P.Rodríguez-Hernández, A.Muñoz, U.R.Rodríguez-Mendoza, V.Lavín, R.J.Angel, J.Gonzalez-Platas. *Inorg. Chem.*, **55**, 7476 (2016)
164. J.Conesa-Egea, J.González-Platas, U.R.Rodríguez-Mendoza, J.I.Martínez, O.Pilar, V.Fernández-Moreira, R.D.Costa, J.Fernández-Cestau, F.Zamora, P.Amo-Ochoa. *J. Mater. Chem. C*, **8**, 1448 (2020)
165. B.Huitorel, R.Utrera-Melero, F.Massuyeau, J.-Y.Mevelec, B.Baptiste, A.Polian, T.Gacoin, C.Martineau-Corcos, S.Perruchas. *Dalton Trans.*, **48**, 7899 (2019)
166. J.Conesa-Egea, J.Gallardo-Martínez, S.Delgado, J.I.Martínez, J.Gonzalez-Platas, V.Fernández-Moreira, U.R.Rodríguez-Mendoza, P.Ocón, F.Zamora, P.Amo-Ochoa. *Small*, **13**, 1700965 (2017)
167. K.N.Jarzembska, R.Kamiński, K.F.Dziubek, M.Citroni, D.Paliwoda, K.Durka, S.Fanetti, R.Bini. *Inorg. Chem.*, **57**, 8509 (2018)
168. S.Keller, A.Prescimone, H.Bolink, M.Sessolo, G.Longo, L.Martínez-Sarti, J.M.Junquera-Hernández, E.C.Constable, E.Ortí, C.E.Housecroft. *Dalton Trans.*, **47**, 14263 (2018)
169. A.A.García-Valdivia, F.J.Romero, J.Cepeda, D.P.Morales, N.Casati, A.J.Mota, L.A.Zotti, J.J.Palacios, D.Choquesillo-Lazarte, J.F.Salmerón, A.Rivadeneyra, A.Rodríguez-Diéguez. *Chem. Commun.*, **56**, 9473 (2020)
170. S.Racioppi, M.Andrzejewski, V.Colombo, A.Sironi, P.Macchi. *Inorg. Chem.*, **59**, 2223 (2020)
171. G.J.Halder, K.W.Chapman, J.A.Schlueter, J.L.Manson. *Angew. Chem., Int. Ed.*, **50**, 419 (2011)
172. N.Hirao, S.I.Kawaguchi, K.Hirose, K.Shimizu, E.Ohtani, Y.Ohishi. *Matter Radiat. Extrem.*, **5**, 018403 (2020)
173. S.A.Moggach, I.D.H.Oswald. In *21st Century Challenges in Chemical Crystallography I. Structure and Bonding*, Vol. 185. (Eds D.M.P.Mingos, P.R.Raithby). (Cham: Springer, 2020). P. 141
174. A.Etcheverry-Berrios, S.Parsons, K.V.Kamenev, M.R.Probert, S.A.Moggach, M.Murrie, E.K.Brechin. *Magnetochemistry*, **6**, 32 (2020)
175. R.A.Davidson, J.S.Miller. *Dalton Trans.*, 2021, **50**, 13859 (2021)
176. J.G.Richardson, A.Mizuno, Y.Shuku, K.Awaga, N.Robertson, C.A.Morrison, M.R.Warren, D.R.Allan, S.A.Moggac. *CrystEngComm*, **23**, 4444 (2021)
177. M.Kazmierczak, E.Patyk-Kazmierczak, A.Katrusiak. *Cryst. Growth Des.*, **21**, 2196 (2021)
178. C.Lecourt, Y.Izumi, K.Maryunina, K.Inoue, N.Belanger-Desmarais, C.Reber, C.Desroches, D.Luneau. *Chem. Commun.*, 57, 2376 (2021)
179. M.Reczyński, D.Pinkowicz, K.Nakabayashi, C.Näther, J.Stanek, M.Kozieł, J.Kalinowska-Tłuścik, B.Sieklucka, S.Ohkoshi, B.Nowicka. *Angew. Chem., Int. Ed.*, 60, 2330 (2021)